THE EUROPEAN
PHYSICAL JOURNAL C

Search for long-lived particles decaying to leptons with large impact parameter in proton–proton collisions at $\sqrt{s} = 13$ TeV

CMS Collaboration[*]

CERN, 1211 Geneva 23, Switzerland

Abstract   A search for new long-lived particles decaying to leptons using proton–proton collision data produced by the CERN LHC at $\sqrt{s} = 13$ TeV is presented. Events are selected with two leptons (an electron and a muon, two electrons, or two muons) that both have transverse impact parameter values between 0.01 and 10 cm and are not required to form a common vertex. Data used for the analysis were collected with the CMS detector in 2016, 2017, and 2018, and correspond to an integrated luminosity of 118 (113) fb^{-1} in the ee channel (eμ and μμ channels). The search is designed to be sensitive to a wide range of models with displaced eμ, ee, and μμ final states. The results constrain several well-motivated models involving new long-lived particles that decay to displaced leptons. For some areas of the available phase space, these are the most stringent constraints to date.

1 Introduction

To date, no evidence of particles beyond the standard model (BSM) has been found by any experiment, including those at the CERN LHC. However, the vast majority of LHC searches assume the lifetimes of new particles are short enough that their decay products are prompt, i.e., their decay products are consistent with originating at the primary proton–proton (pp) interaction. Search strategies are rarely optimized for particles with measurable lifetimes whose decays produce detector signatures that are displaced from the primary pp interaction. Therefore, new phenomena with displaced signatures can escape such searches. Particles in BSM scenarios can have long lifetimes for the same reasons as standard model (SM) particles, namely, small couplings between the long-lived particles (LLPs) and lighter states, approximate symmetries, heavy intermediate states, or limited phase space availability for decays.

While the majority of searches are only sensitive to models that predict new phenomena with prompt signatures, the ATLAS, CMS, and LHCb Collaborations have performed dedicated searches for decays of BSM particles with long lifetimes. Direct search strategies include finding BSM particles via their anomalous energy loss and/or low velocity [1,2] or via a disappearing track signature [3–5]. There are also numerous indirect searches targeting the decay products of LLPs, such as nonprompt final-state jets [6–12], photons [13,14], leptons [15–21], or combinations thereof [22–25]. These searches are often complementary, providing sensitivity to different ranges of particle lifetimes and masses.

The CMS Collaboration has previously performed a search for signatures with one displaced electron and one displaced muon, using pp collision data recorded at $\sqrt{s} = 8$ TeV and corresponding to an integrated luminosity of 19.7 fb^{-1} [26]. Both this previous analysis and the one described in this paper, which uses data recorded at $\sqrt{s} = 13$ TeV, are optimized to the phase space just beyond the sensitivity of prompt searches but with smaller displacements than other searches for long-lived BSM signatures. As a result, this search is sensitive to LLPs with proper decay lengths ($c\tau_0$) between approximately 10^{-3} and 10^3 cm, where c is the speed of light and τ_0 is the proper lifetime. These two analyses are unique in that they allow but do not require the displaced final-state particles to originate from a common vertex. Such a vertex is often required in other searches under the assumption that an LLP will decay to multiple leptons. In contrast, here we perform an inclusive search that is sensitive to one LLP that decays to multiple leptons, two LLPs that each decay to at least one lepton, and any other topology whose final state includes at least two displaced leptons. The search described in this paper uses data taken with the CMS detector during 2016, 2017, and 2018. We conduct a search for events in which there are one electron and one muon, two electrons, or two muons in the final state, where both of the leptons are displaced from the beam axis. With respect to the previous search, this search is based on about a factor of 6 larger integrated luminosity, is performed at a higher $\sqrt{s}$, and adds two same-flavor channels corresponding to the ee and μμ final states.

*[*] e-mail: cms-publication-committee-chair@cern.ch

This search is designed to be model independent and to be sensitive to as many event topologies as possible. Consequently, the event selection focuses exclusively on a displaced, isolated dilepton signature and does not try to identify signal events using hadronic activity or missing transverse momentum from undetected particles. In this way, we retain sensitivity to any model that can produce leptons with displacements on the order of 0.01 to 10 cm and with sufficiently high momenta, regardless of whether these leptons are accompanied by jets, missing transverse momentum, or other kinematic features.

We interpret the search results in the context of several models that produce final states with displaced leptons, the Feynman diagrams for which are shown in Fig. 1. The first model introduces R-parity-violating (RPV) terms in the superpotential of the minimally supersymmetric (SUSY) SM [27], allowing the lightest SUSY particle (LSP) to decay to SM particles. Only lepton-number-violating operators are considered because of constraints from measurements of the lifetime of the proton [28]. With sufficiently small couplings for these operators, the LSP has a long enough lifetime that its decay products are measurably displaced from the pp interaction region. We focus on the case in which the LSP is the top squark $(\widetilde{t})$, the superpartner of the top quark. At the LHC, the top squark would be dominantly pair produced, and we consider its decay through an RPV vertex to a d (b) quark and a charged lepton ℓ via $\widetilde{t} \to d\ell$ $(\widetilde{t} \to b\ell)$. With respect to the previous analysis [26], we have added the $\widetilde{t} \to d\ell$ decay to facilitate reinterpreting the results in a wider range of BSM scenarios, although we find that this decay mode produces similar results to those from the $\widetilde{t} \to b\ell$ decay. We expect that the $\widetilde{t} \to s\ell$ decay mode will also produce similar results, although we did not explore it. For simplicity, we assume lepton universality in the top squark decay vertex, so that the branching fraction to any lepton flavor, namely, an electron, muon, or tau lepton, is equal to one-third. We also interpret the results with a gauge-mediated SUSY breaking (GMSB) model in which the next-to-lightest SUSY particle (NLSP) is long lived because of its small gravitational coupling to the LSP gravitino $\widetilde{G}$, which is nearly massless [29]. In this model, the NLSP is the superpartner of a lepton (slepton $\widetilde{\ell}$). We consider selectrons $\widetilde{e}$, smuons $\widetilde{\mu}$, and staus $\widetilde{\tau}$ separately, as well as together, as co-NLSPs. The sleptons would be pair produced at the LHC and each would decay to a lepton (e, μ, or τ) of the same flavor and a gravitino. In addition, we consider a model that produces BSM Higgs bosons (H) with a mass of 125 GeV through gluon–gluon fusion [30]. The H decays to two long-lived scalars S, each of which decays to two oppositely charged and same-flavor leptons, and the probabilities of the lepton pair being ee or $\mu\mu$ are assumed to be the same. For the scenarios where the long-lived top squarks and sleptons decay to tau leptons, events in which the tau leptons both subsequently decay into electrons or muons are considered.

Tabulated results are provided in the HEPData record for this analysis [31].

2 The CMS detector

The central feature of the CMS apparatus is a superconducting solenoid of 6 m internal diameter, providing a magnetic field of 3.8 T. Within the solenoid volume are a silicon pixel and strip tracker, a lead tungstate crystal electromagnetic calorimeter (ECAL), and a brass and scintillator hadron calorimeter, each composed of a barrel and two endcap sections. The electron momentum is estimated by combining the energy measurement in the ECAL with the momentum measurement in the tracker. Forward calorimeters extend the pseudorapidity η coverage provided by the barrel and endcap detectors. Muons are measured in gas-ionization detectors embedded in the steel flux-return yoke outside the solenoid using three technologies: drift tubes (DTs) in the barrel, cathode strip chambers (CSCs) in the endcaps, and resistive-plate chambers in both the barrel and the endcaps. Each of the four muon detector planes provides reconstructed hits on several detection layers, which are combined into local track segments, forming the basis of muon reconstruction inside the muon system.

The silicon tracker measures charged particles with $|\eta| < 3.0$. During the 2016 LHC run, the silicon tracker consisted of 1440 silicon pixel and 15 148 silicon strip detector modules. The pixel detector was then upgraded, such that in the 2017 and 2018 LHC runs, it consisted of 1856 pixel modules. After the upgrade, the number of pixel layers increased from three, with radii between 4.4 and 10.2 cm from the interaction region, to four, with radii between 2.9 and 16.0 cm [32]. In the 2017 and 2018 LHC runs, for nonisolated particles within the transverse momentum range $1 < p_T < 10$ GeV and $|\eta| < 3.0$, the average track p_T resolution is 1.5%. The transverse impact parameter (d_0) is defined as the distance of closest approach in the transverse plane of the helical trajectory of the track with respect to the beam axis [33,34]. The sign of d_0 is given by the sign of the scalar product between the lepton momentum and the vector from the beam axis to the lepton track reference point. The track d_0 resolution improves from 75 to 20 μm as the p_T increases, for nonisolated particles with $1 < p_T < 10$ GeV and $|\eta| < 3.0$ in 2017 and 2018. With the upgraded silicon pixel tracker, the d_0 resolution is approximately 25% better than in earlier data sets. The efficiency to reconstruct tracks as a function of $|d_0|$ is given in Ref. [34].

Events of interest are selected using a two-tiered trigger system. The first level, composed of custom hardware processors, uses information from the calorimeters and muon

Fig. 1 Feynman diagrams for $\widetilde{t} \to b\ell$ (upper left), $\widetilde{t} \to d\ell$ (upper right), $\widetilde{\ell} \to \ell\widetilde{G}$ (lower left), and $H \to SS$, $S \to \ell^+\ell^-$ (lower right)
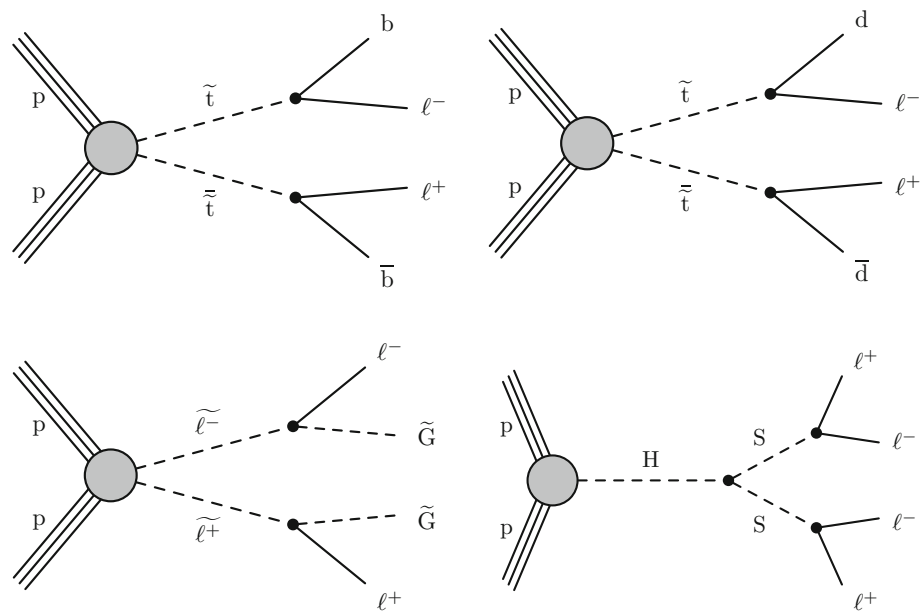
detectors to select events at a rate of around 100 kHz within a fixed latency of about 4 μs [35]. The second level, known as the high-level trigger (HLT), consists of a farm of processors running a version of the full event reconstruction software optimized for fast processing, and reduces the event rate to around 1 kHz before data storage [36,37].

A more detailed description of the CMS detector, together with a definition of the coordinate system used and the relevant kinematic variables, can be found in Ref. [38].

3 Data and Monte Carlo simulation

The data correspond to an integrated luminosity of 118 (113) fb^{-1} in the ee channel (eμ and μμ channels), 16 fb^{-1} of which were collected in 2016 before the pixel detector upgrade. The difference in integrated luminosity in the different channels is due to the availability of the triggers, which will be described in Sect. 5. In addition, we use events containing muons from cosmic ray showers that were recorded with dedicated triggers for a control sample to evaluate the tracking efficiency of displaced particles, as will be described later.

In the Monte Carlo (MC) simulation of background and signal processes, minimum-bias interactions are superimposed on each event to simulate the effect of additional interactions within the same or neighboring bunch crossing (pileup). The frequency distribution of the additional interactions is adjusted to match that observed in data. The average number of pileup interactions was 23 (32) in 2016 (2017 and 2018). For the 2016 samples, the NNPDF3.0 [39] parton distribution function (PDF) set at next-to-leading order

(NLO) is used, while for the samples describing the 2017 and 2018 data, the NNPDF3.1 PDF set computed at next-to-NLO order [40] is used. The PYTHIA generator is used to simulate the parton showering and hadronization for all processes. The modeling of the underlying event uses PYTHIA 8.226 [41] with the CUETP8M1 [42] tune and PYTHIA 8.230 with the CP5 tune [43] for simulated samples corresponding to the 2016 and 2017–2018 data sets, respectively. The MC-generated events are then processed through a detailed simulation of the CMS detector based on GEANT4 [44] and are reconstructed with the same algorithms used for data.

While the background is estimated using data control samples, simulated background samples are produced to perform basic checks such as comparisons of data and simulation in control regions (CRs). Samples of simulated Z+jets, W+jets, and t$\bar{\text{t}}$ production are generated at leading order (LO) using MADGRAPH5_aMC@NLO v2.2.2 (v2.4.2) for the 2016 (2017 and 2018) samples [45] and the MLM merging scheme between jets from matrix element calculations and parton showers [46]. Samples of diboson and single top quark events are simulated at NLO with POWHEG v2.0 [47–51]. Quantum chromodynamics (QCD) multijet events, which give rise to a background from SM events composed uniquely of jets produced through the strong interaction, are simulated with PYTHIA, selecting events that are enriched in muons. Samples of the signal process pp $\to \widetilde{t}\widetilde{\bar{t}}$, with the top squarks decaying via $\widetilde{t} \to d\ell$ or $\widetilde{t} \to b\ell$, are generated using PYTHIA at LO. The top squarks can form strongly produced hadronic states called R-hadrons, which are generated with PYTHIA. In the samples used in this analysis, the interactions of the R-hadrons with matter are not simulated in GEANT4. However, such interactions are not expected to have a significant

impact because these particles do not encounter a significant number of interaction lengths before decaying. Nevertheless, we study the impact of the R-hadron interactions using the "cloud model," which assumes that the top squark is surrounded by a cloud of colored, light constituents that interact during scattering [52,53], and find the effect on the signal efficiency to be negligible. The GMSB sleptons are generated at LO using MADGRAPH5_aMC@NLO v2.6.5 and PYTHIA, and the slepton decay via $\widetilde{\ell} \to \ell\widetilde{G}$ is simulated using GEANT4, which ignores information about the chirality of the slepton. Thus, we do not present results for left- and right-handed sleptons separately. The signal process $pp \to H \to SS$, $S \to \ell^+\ell^-$ is generated using POWHEG and PYTHIA at NLO.

4 Analysis strategy

We perform an inclusive search for displaced leptons by selecting events with well-reconstructed electrons and muons, and by rejecting background events from SM processes that produce displaced leptons, as will be described in Sect. 5. We use the lepton $|d_0|$, which is the main discriminating variable in the analysis, to define the signal regions (SRs). Using data in a prompt CR, we correct the $|d_0|$ distributions in the background and signal simulations to account for alignment and resolution effects that are not fully modeled in the simulations; this procedure will be presented in Sect. 6. Section 7 describes how we perform a background estimate based on control samples in data, using the lepton $|d_0|$ to separate signal-like events from background-like ones. Because the lepton $|d_0|$ distributions for the signal processes are modeled with simulation, we validate the modeling of the displaced tracking efficiency in data using displaced muons from cosmic ray events. Section 8 describes how, from these studies, we derive systematic uncertainties that are applied to the signal.

5 Event reconstruction and selection

Events were recorded with different triggers in each of the three channels. Because standard CMS electron triggers are not designed to recognize displaced tracks, we use photon triggers instead to ensure efficiency for finding displaced electrons. In fact, photon HLT paths efficiently select electrons as well, as these triggers do not veto electrons or charged particle tracks. In the eµ channel, the trigger requires at least one muon candidate that is not constrained to the primary pp interaction vertex and without any maximum $|d_0|$ requirement, and at least one photon candidate. In 2016 data, the muon and photon candidates are both required to have $p_T > 28$ GeV if the muon candidate $|d_0|$ is greater than 0.01 cm, and $p_T > 38$ GeV otherwise. In 2017 and 2018

data, the muon and photon candidates are both required to have $p_T > 43$ GeV; the p_T threshold was increased between the 2016 and 2017 data-taking periods to mitigate the effects of the increased pileup. In the ee channel, the events are required to pass at least one of two HLT paths. The first HLT path simply requires at least two photon candidates with $p_T > 60$ (70) GeV in 2016 (2017 and 2018) data. The second HLT path, which is included to partially recover events with lower p_T electrons, requires the highest p_T photon candidate to have $p_T > 30$ GeV and the second-highest p_T photon candidate to have $p_T > 18$ (22) GeV in 2016 (2017 and 2018) data. The photon candidates passing this second trigger must satisfy requirements based on calorimeter cluster shape, isolation, and the ratio of the hadronic to electromagnetic energy, and the diphoton invariant mass must be >90 GeV. In the µµ channel, the trigger requires at least two muon candidates without any primary vertex constraints and without any maximum requirement on the impact parameter. In 2016 data, the muon candidates are required to have $p_T > 23$ GeV if the muon candidate $|d_0|$ is greater than 0.01 cm, and $p_T > 33$ GeV otherwise. In 2017 and 2018 data, the muon candidates are required to have $p_T > 43$ GeV. For the masses and lifetimes we consider, the efficiency for signal events to pass these triggers is 20–40%, depending on mass, lifetime, analysis channel, and year.

After requiring that the events pass the triggers described above, we preselect well-reconstructed electrons and muons in each channel. Electrons and muons are reconstructed by associating a track reconstructed in the tracking detectors with either a cluster of energy in the ECAL [54,55] or a track in the muon system [56]. The leptons used in this search are reconstructed with the particle-flow (PF) algorithm [57], which aims to reconstruct and identify each individual particle in an event with an optimized combination of information from the various elements of the CMS detector. The primary pp interaction vertex is taken to be the candidate vertex with the largest value of summed physics-object p_T^2. The physics objects used for this determination are the jets, clustered using the jet finding algorithm [58,59] with the tracks assigned to candidate vertices as inputs, and the associated missing transverse momentum, taken as the negative vector sum of the p_T of those jets.

In the eµ channel, we preselect events with at least one PF electron and at least one PF muon, while in the same-flavor channels, we preselect events with at least two PF electrons or muons. To retain sensitivity to signals that could produce leptons with the same charge, we make no requirements on the charge of the leptons. In the eµ channel, we require the electrons to have $p_T > 42$ (45) GeV and the muons to have $p_T > 40$ (45) GeV in 2016 (2017 and 2018). In the ee channel, we require the electrons to have $p_T > 65$ (75) GeV, and in the µµ channel, we require the muons to have $p_T > 35$ (45) GeV. These p_T requirements ensure that the trigger effi-

ciencies do not depend on p_T. In all three channels, we require the electrons and muons to have $|\eta| < 1.5$ in order to remove leptons with poorly measured $|d_0|$, which would be predominantly at high $|\eta|$. Since the signal leptons in the benchmark models are predominantly central, this requirement has a minimal impact on the signal efficiencies. In addition, electrons in the ECAL transition region between the barrel and endcap detectors are rejected because the electron reconstruction in this region is not optimal. This criterion effectively means that electrons are required to have $|\eta| < 1.44$. We also reject electrons and muons in certain regions of the η-ϕ plane, where ϕ is the azimuthal angle, because two layers of the pixel tracker were not fully functional during certain data-taking periods, resulting in increased $|d_0|$ mismeasurements. The rejected regions are $1.0 < \eta < 1.5, 2.7 < \phi \leq \pi$ in 2017 and $0.3 < \eta < 1.2, 0.4 < \phi < 0.8$ in 2018. This requirement reduces the relative signal efficiency by $<1\%$, and so we apply it for the entire 2017 and 2018 data-taking periods.

Identification requirements, based on energy deposits in the calorimeters and on hit information in the tracker and muon systems, are imposed on the electrons and muons at the "tight" working point [54–56]. Included in these identification requirements is the criterion that at least one of the first two functional pixel layers traversed by the electron must register a hit. The identification requirements for muons include that each muon track must have at least one hit in the pixel detector, at least six tracker layer hits, and segments with hits in two or more muon detector stations.

To ensure that electrons and muons are isolated from other particles, we calculate the scalar p_T sum of all other particles around the electron (muon) within a cone of $\Delta R \equiv \sqrt{(\Delta\eta)^2 + (\Delta\phi)^2} < 0.3$ (0.4), correct this sum for contributions from pileup, and define the relative isolation as the ratio of this sum to the electron (muon) p_T. For each lepton, the pileup correction term is calculated as the area of the lepton's isolation cone multiplied by the average energy per unit area in η-ϕ space in the event. By including objects from any vertex in the isolation sum, we allow for the possibility that the displaced lepton is associated with the wrong primary vertex. We require that the relative isolation is <0.10 for muons, <0.0588 for electrons in 2016, and $<0.0287 + 0.506\,\mathrm{GeV}/p_T$ for electrons in 2017 and 2018.

Besides these object-level selections, we also impose several event-level selections. To remove cosmic ray muons in the $\mu\mu$ and $e\mu$ channels, we require that there are zero pairs of muons with $\cos\alpha < -0.99$, where α is the three-dimensional angle between the muons. This selection removes back-to-back muons, which is how cosmic ray muons from the Earth's atmosphere appear in the detector. In addition, we require that the relative time between the leading (largest p_T) two muons is not consistent with the timing of cosmic ray muons. To determine the time associated with each muon, we propa-

gate the signal times as measured in the DTs and CSCs to the beam axis assuming the muons are outgoing. We then determine which muon is above the other based on their ϕ measurements and find Δt, the time of the lower muon subtracted from the time of the upper muon. Since cosmic ray muons traverse the detector from top to bottom, the lower muon appears later in time than the upper muon, assuming the muons are outgoing from the beam axis, making Δt negative for cosmic ray muons. On the other hand, muons from the pp collision have similar times as they are both outgoing from the beam axis, and so they have a Δt distribution centered at 0 ns. We reject events with $\Delta t < -20$ ns if there are at least eight independent time measurements to determine the time of flight of each muon. We also require that the relevant leptons in each channel are separated by $\Delta R > 0.2$. This loose requirement is sufficient to significantly reduce the contribution of the heavy-flavor background from cascade decays of b or c hadrons. To remove pairs of leptons from material interactions, we reject events where the candidate leptons form a good displaced vertex that overlaps with the tracker material, which is measured in Ref. [60]. The vertices are reconstructed with the Kalman vertex fitter [61,62], and a "good" vertex is one with a position uncertainty of less than $10\,\mu\mathrm{m}$ and a $\chi^2/N_{\mathrm{dof}} < 20$, where N_{dof} is the number of degrees of freedom of the fit.

The events satisfying the preselection criteria for each channel are further categorized using the $|d_0|$ of the selected leptons. We define a "prompt CR" by requiring the electrons and muons to have $|d_0| < 50\,\mu\mathrm{m}$. This region is dominated by SM processes with prompt leptons and is used to check that the background simulation accurately reproduces the behavior of the data. The "inclusive SR" is defined by requiring the electrons and muons have $100\,\mu\mathrm{m} < |d_0| < 10$ cm. We do not select leptons that are displaced by more than 10 cm to ensure that the leptons originate within the pixel tracker, since the lepton identification criteria require hits in at least one pixel layer.

To remove overlaps among the three channels, events that pass the $e\mu$ inclusive SR selection are rejected from the same-flavor channels.

Table 1 shows the cumulative signal efficiency for several choices of $\tilde{t}$ mass and $c\tau_0$. The efficiencies are similar for each year of data taking. The larger signal efficiency in the $e\mu$ channel relative to either of the same-flavor channels occurs primarily because two top squarks decaying with equal probability to an electron, a muon, or a tau lepton will produce an $e\mu$ final state twice as often as either of the same-flavor final states.

Table 1 The cumulative efficiencies for $\tilde{t} \to b\ell$ signal events to pass the 2018 inclusive SR selection, for several choices of $\tilde{t}$ mass (columns) and $c\tau_0$ (rows). For each entry, the numerator is the weighted number of events passing the SR selection, and the denominator is the total weighted number of generated signal events. The corrections described in Sect. 6 are applied

	200 GeV	1000 GeV	1800 GeV
eμ SR			
0.1 cm	2.0%	4.5%	4.5%
1 cm	3.5%	7.8%	8.7%
10 cm	1.0%	2.6%	3.3%
100 cm	0.05%	0.12%	0.15%
ee SR			
0.1 cm	0.45%	2.1%	2.1%
1 cm	0.59%	2.8%	3.3%
10 cm	0.11%	0.59%	0.76%
100 cm	0.002%	0.01%	0.02%
μμ SR			
0.1 cm	1.4%	2.5%	2.5%
1 cm	3.0%	5.5%	5.8%
10 cm	1.4%	3.0%	3.6%
100 cm	0.10%	0.22%	0.31%

6 Corrections to the simulation

Several corrections are applied to the MC simulations in order to account for the known differences between simulation and data. The simulation is corrected so that its distribution of pileup interactions matches that of 2016, 2017, and 2018 data. In addition, the trigger efficiency is measured in simulation and in an independent data sample recorded with missing p_T triggers, for the three data-taking years and for each analysis channel separately. The ratio of the trigger efficiency in data and simulation is applied as a "scale factor" to each event in the simulated samples. Averaged over the years, the trigger scale factors for the eμ, ee, and μμ channels are 0.94 ± 0.01, 1.00 ± 0.17, and 0.88 ± 0.01, respectively. While these trigger scale factors are derived with samples dominated by prompt events, we also evaluate consistent scale factors when the leptons in these samples are required to be displaced. Scale factors are also applied as functions of lepton p_T and η in order to correct the performance of the lepton identification and isolation algorithms [54–56].

Corrections are also applied to each lepton in order to make the simulated lepton $|d_0|$ distributions match those in data, in prompt CRs. These corrections are derived by fitting the simulated background and the data lepton d_0 distributions with Gaussian functions in each channel's prompt CR, and by then comparing the widths of the Gaussian functions. The width of each Gaussian function is largely set by the lepton d_0 resolution, and the discrepancy between the data and

background MC simulation lepton d_0 distributions is largely due to an overly optimistic alignment in the simulation, which creates an unrealistically precise d_0 resolution. Therefore, we define $\sigma_{\text{data}}^2 = \sigma_{\text{bkg}}^2 + \sigma_{\text{correction}}^2$, where σ_{data} is the width of the function fit to data, σ_{bkg} is the width in background simulation, and $\sigma_{\text{correction}}$ is the additional piece that is needed to make the background simulation and data agree in each channel's prompt CR. We find σ_{data} and σ_{bkg} from the fits, and compute $\sigma_{\text{correction}}$. Because the fit results are similar in each channel, we average the $\sigma_{\text{correction}}$ derived in the ee and eμ channels for electrons, and in the μμ and eμ channels for muons. We then smear the simulated d_0 distribution by picking random values within a Gaussian distribution centered at 0 and with a width of the average $\sigma_{\text{correction}}$, and applying these random values as corrections to each lepton d_0. The average $\sigma_{\text{correction}}$ is 14.8 ± 0.4 (9.2 ± 0.4) μm for electrons and 7.6 ± 0.1 (8.1 ± 0.1) μm for muons in 2017 (2018). No $|d_0|$ correction is found to be needed for the simulation with 2016 data-taking conditions, as the simulation for 2016 data already has refined alignment conditions that match the data. The corrections are applied to both background and signal MC simulation.

7 Background estimation

Most leptons resulting from SM processes originate in prompt particle decays. However, displaced leptons can arise from several different sources. Displaced leptons resulting from cosmic ray muons, material interactions, and long-lived SM hadrons are largely rejected by the analysis selection criteria. The tight isolation criterion is particularly useful in rejecting the vast majority of the heavy-flavor background. Nevertheless, leptons from mismeasurements of prompt tracks or from decays of tau leptons, which have a mean $c\tau_0$ value of 87 μm, and long-lived hadrons such as B and D mesons, which have mean $c\tau_0$ values of 500 and <100 μm, respectively, may still appear in the SRs.

7.1 The ABCD method

To estimate the number of background events in the SRs, we employ an "ABCD method" based on control samples in data that account for all three significant background sources: mismeasurements, tau lepton decays, and heavy-flavor decays. First, we categorize the events that pass the preselection criteria into four regions (A, B, C, and D) based on each lepton $|d_0|$ measurement, namely, $|d_0^a|$ and $|d_0^b|$, as shown in Fig. 2. For the eμ channel, $|d_0^a|$ is defined as the leading electron $|d_0|$ and $|d_0^b|$ is defined as the leading muon $|d_0|$. For the ee (μμ) channel, $|d_0^a|$ is defined as the leading electron (muon) $|d_0|$ and $|d_0^b|$ is defined as the subleading electron (muon) $|d_0|$. We use the number of background events in regions A, B, and
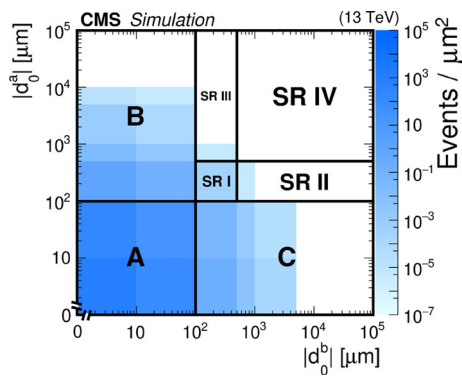
Fig. 2 A diagram of the ABCD method, shown for illustration on simulated background events passing the eμ preselection with 2018 conditions. In each $|d_0^a|$-$|d_0^b|$ bin, the number of events divided by the bin area is plotted. A, B, and C are CRs. SRs I–IV are described in Sect. 7.2

C to estimate the expected background in region D, which is the SR. We start from the assumption that $N_B/N_A = N_D/N_C$ so that the number of background events in D is $N_B N_C/N_A$, where N_X is the number of background events in the given region. This assumption is valid if $|d_0^a|$ and $|d_0^b|$ are statistically independent. We identify deviations from this assumption using the closure tests described in Sect. 7.3 and correct for them using the procedure described in Sect. 7.4.

7.2 Signal regions

We subdivide the inclusive SR to define nonoverlapping SRs in $|d_0|$:

– SR I: $100 <$ both $|d_0| < 500\,\mu\text{m}$
– SR II: $100 < |d_0^a| < 500\,\mu\text{m}$, $500\,\mu\text{m} < |d_0^b| < 10\,\text{cm}$
– SR III: $500\,\mu\text{m} < |d_0^a| < 10\,\text{cm}$, $100 < |d_0^b| < 500\,\mu\text{m}$
– SR IV: $500\,\mu\text{m} <$ both $|d_0| < 10\,\text{cm}$

We also split SR I, which has the largest number of expected background events, into two bins. In the eμ and $\mu\mu$ channels, these bins are in the leading muon p_T, and in the ee channel, these bins are in the leading electron p_T. The bin boundary is at 90 (140) GeV for the 2016 (2017 + 2018) eμ channel, at 300 (400) GeV for the 2016 (2017 + 2018) ee channel, and at 100 GeV for all years in the $\mu\mu$ channel. The p_T bins are chosen such that the bin with higher p_T contains less than one expected background event, which maximizes the sensitivity to short lifetimes.

Dividing the inclusive SR in this way separates the expected contribution of different background sources into individual SRs, and gives loose SRs with some amount of background contamination but high signal efficiency and tight SRs with little background contamination but also smaller signal efficiency. The signal efficiency in each SR

depends on the lifetime of the LLP, so dividing the inclusive SR into multiple SRs also helps the search to be sensitive to a wide range of LLP lifetimes. Because they are nonoverlapping, we can use these SRs simultaneously in the signal extraction procedure.

We perform a separate ABCD estimate for each SR. When performing the estimates, we subdivide regions B and C into 100–500$\,\mu\text{m}$ and 500$\,\mu\text{m}$–10 cm regions to match the SR definitions, and subdivide region A and the 100–500$\,\mu\text{m}$ subregions of B and C in p_T to match the binning of SR I.

7.3 Closure tests in one-prompt/one-displaced sidebands

The background estimation method starts from the premise that the lepton $|d_0|$ values are independent. The preselection criteria remove one possible source of dependence between the $|d_0|$ values by ensuring that leptons that share a common displaced vertex do not contribute meaningfully to the SRs, but dependence between the $|d_0|$ values may still arise from processes in which the leptons originate from the same type of parent particle. Specifically, we find that $Z \to \tau\tau$ events in which each tau lepton decays to an electron or muon lead to a dependence between the lepton $|d_0|$ values, since each electron or muon is produced in the decay of a long-lived tau lepton. In principle, processes that produce pairs of b or c hadrons could introduce dependence between the $|d_0|$ values through this same mechanism, but the lepton isolation criteria ensure a negligible SR contribution from events in which both leptons are produced in b or c hadron decays. We therefore expect the degree of $|d_0|$ dependence to increase with the fraction of events from $Z \to \tau\tau$. Studies with simulation show that leptons from tau lepton decays contribute significantly from about 100–500$\,\mu\text{m}$ and peak around 200$\,\mu\text{m}$, so we expect the $|d_0|$ dependence to appear in this range and peak accordingly. Thus, the background contribution from leptons from tau lepton decays is confined to SR I. The ability to measure such dependence between the $|d_0|$ values depends on the quality of the $|d_0|$ measurement. Because $|d_0|$ resolution is better for muons than for electrons and is better in the 2017 and 2018 data-taking periods relative to the 2016 data-taking period, we also expect the dependence between the $|d_0|$ values to be more apparent in 2017 and 2018 and to increase with the number of muons in the final state. We observe this dependence between the $|d_0|$ values in the closure tests described below and correct for it using the procedure described in Sect. 7.4.

We perform closure tests in sideband regions that are orthogonal to the SRs, in data and background simulation. These sideband regions have one prompt and one displaced lepton. We first perform these closure tests in the region where the prompt (displaced) lepton has a displacement of 30–100 (100–500)$\,\mu\text{m}$. We use the estimated and actual yields in several subregions of each sideband region to esti-

Table 2 Closure test results in data, background simulation, and background simulation with the $Z \rightarrow \tau\tau$ events removed in the 100–500 μm region. The extrapolated ratios of the actual yield to the estimated yield (averaged over the two one-prompt/one-displaced sidebands) and their statistical uncertainties are given

Year and channel	Data	Full bkg. simulation	Bkg. sim. w/o $Z \rightarrow \tau\tau$
2016 eμ	0.9 ± 1.3	1.6 ± 0.6	0.9 ± 0.3
2017+2018 eμ	3.1 ± 0.8	1.6 ± 0.7	1.1 ± 0.4
2016 ee	0.6 ± 0.6	0.8 ± 0.5	0.8 ± 0.5
2017+2018 ee	1.5 ± 0.4	1.6 ± 0.9	0.8 ± 1.0
2016 μμ	2.5 ± 0.9	2.0 ± 0.8	1.1 ± 0.8
2017+2018 μμ	4.2 ± 1.5	7.8 ± 3.7	2.6 ± 2.8

Table 3 Closure test results in data, background simulation, and background simulation with the $Z \rightarrow \tau\tau$ events removed in the 500 μm–10 cm region. The ratios of the actual yield to the estimated yield (averaged over the two one-prompt/one-displaced sidebands) and their statistical uncertainties are given

Year and channel	Data	Full bkg. simulation	Bkg. sim. w/o $Z \rightarrow \tau\tau$
2016 eμ	$0.4^{+1.0}_{-0.4}$	$1.0^{+0.3}_{-0.2}$	$1.0^{+0.3}_{-0.2}$
2017+2018 eμ	$0.7^{+0.7}_{-0.4}$	$0.9^{+0.2}_{-0.1}$	$0.8^{+0.2}_{-0.2}$
2016 ee	$1.0^{+0.9}_{-0.5}$	$2.2^{+2.9}_{-1.6}$	$2.2^{+2.9}_{-1.5}$
2017+2018 ee	$1.0^{+0.2}_{-0.2}$	$1.2^{+1.3}_{-0.7}$	$2.0^{+1.4}_{-0.9}$
2016 μμ	$0.7^{+0.3}_{-0.2}$	$1.0^{+0.3}_{-0.3}$	$0.9^{+0.3}_{-0.2}$
2017+2018 μμ	$1.2^{+0.3}_{-0.4}$	$0.5^{+0.6}_{-0.2}$	$0.6^{+0.9}_{-0.4}$

mate the ratio of the actual yield to the estimated yield in SR I. This procedure will be described in more detail in Sect. 7.4. Table 2 shows the resulting ratios in data, background simulation, and background simulation with the $Z \rightarrow \tau\tau$ events from the Z+jets samples removed. As expected, the ratios in data are frequently greater than unity, which indicates nonclosure of the ABCD method and positive $|d_0|$ dependence. The data ratios generally agree with those of the full background simulation, which indicates that the source of nonclosure is modeled in the background simulation. When the $Z \rightarrow \tau\tau$ events are removed from the simulation, we find that the ratios are consistent with unity. Because the full simulation successfully models the observed nonclosure in data and because removing the $Z \rightarrow \tau\tau$ events results in closure, we conclude that $Z \rightarrow \tau\tau$ events are indeed the only meaningful source of $|d_0|$ dependence. We note that the superior $|d_0|$ resolution of the upgraded pixel detector frequently results in fewer events in the sideband regions in 2017 and 2018 data than in 2016 data, which can lead to larger uncertainties in the 2017 + 2018 closure test results shown in Table 2, notably in the μμ channel.

We next perform closure tests in sideband regions where one lepton is prompt (30–100 μm) and the other is even more displaced (500 μm–10 cm). Table 3 shows the ratios of the actual yield to the estimated yield averaged over the two one-prompt/one-displaced sidebands in data, background simulation, and background simulation with the $Z \rightarrow \tau\tau$ events removed. In each case, the resulting ratios are consistent with unity, and data and background simulation agree. Thus, in contrast to the 100–500 μm region tests, the 500 μm–10 cm region tests show no evidence of $|d_0|$ dependence. We also note that removing the $Z \rightarrow \tau\tau$ events from the background

simulation does not significantly affect the results, which provides further evidence that the background from tau lepton decays is small in this region. We therefore conclude that $|d_0|$ dependence is significant in the 100–500 μm region and insignificant in the 500 μm–10 cm region.

7.4 Background estimate correction and systematic uncertainty

We now define a procedure to account for the $|d_0|$ dependence in the ABCD method and assign a systematic uncertainty in the estimate. First, as is done in the closure tests, we divide each one-prompt/one-displaced sideband into two subregions in the displaced lepton $|d_0|$: (1) the 100–500 μm region, where we find $|d_0|$ dependence from tau leptons to be significant, and (2) the 500 μm–10 cm region, where we find $|d_0|$ dependence from tau leptons to be insignificant. The 100–500 μm (500 μm–10 cm) sideband region is used as a CR for SR I (SRs II–IV). We perform closure tests in data in each sideband subregion and use the ratio of the actual to the estimated number of events as a measure of nonclosure.

From the 500 μm–10 cm region tests, we take the largest deviation of the ratio from unity as a systematic uncertainty in SRs II–IV, and apply no correction. This approach produces systematic uncertainties between about 40 and 200% in the background estimates, whose central values range from 0.003 to 3.6 events.

When the displaced lepton $|d_0|$ is between 100 and 500 μm, we fit the ratio as a function of the prompt lepton $|d_0|$ with a straight line, where the slope and y intercept are allowed to vary. We extrapolate the prompt lepton fit to 200 μm (within SR I), which is the value where sim-

ulation indicates we should expect the largest contribution from tau lepton decays. The mean lepton $|d_0|$ of the 100–500 μm bin in the background simulation is also approximately 200 μm. We determine the uncertainty in each extrapolated ratio by simultaneously varying the fit parameters according to their 68% confidence interval, while accounting for correlations between the parameters. We take the average of the two extrapolated ratios (one from each one-prompt/one-displaced sideband) and derive a correction and its systematic uncertainty from this average ratio. If the average is greater than unity, we use the average as a multiplicative correction to the background estimate, and we use the uncertainty in the average as a systematic uncertainty in the background estimate. The uncertainty in the average is obtained through simple uncertainty propagation. In this case, we also vary the 200 μm extrapolation point by $\pm 50\,\mu$m, which is the approximate range of the tau lepton contribution as a function of $|d_0|$, and apply the variation in the resulting correction as an additional systematic uncertainty in the background estimate. If the average is less than or equal to unity, we set the correction equal to unity and use the uncertainty in the average as a symmetric systematic uncertainty about unity. The size of the correction varies between 1.0 ± 0.6 and 4.2 ± 1.8, depending on channel and year.

7.5 Closure tests in SRs

To test the full background estimation procedure, we perform closure tests in background simulation in the four SRs, with all corrections and systematic uncertainties derived from background simulation. In these tests, both leptons are displaced. The results of these closure tests in the SRs are shown in Table 4 with the 2016 and 2017+2018 yields combined in each channel. In this table, the actual and estimated yields are given, as opposed to Tables 2 and 3, which display the ratios. The actual yields are compatible with the estimated yields, which indicates that the correction performs as expected and the systematic uncertainties are sufficient to cover any unforeseen dependency.

7.6 Additional studies

In addition, we perform several studies to check for other potential sources of background in the SRs. First, to check the significance of material interactions, we invert the criterion that rejects material interactions. After doing so, we find no events in the SRs in data, across all channels and years. Thus, we conclude that there is no significant background from material interactions after the full selection criteria are applied. Second, to test for the presence of cosmic ray muon events, we invert the cosmic ray muon rejection criteria in the $\mu\mu$ channel and scale the number of events by the effi-

Table 4 Closure test results in background simulation in the SRs, with the corrections applied. The estimated numbers of events, the actual numbers of events, and their total uncertainties (statistical plus systematic) are given. In cases where the actual number of events is zero, the uncertainty is given by the product of the average background simulation event weight and the upper bound of the 68% confidence level Poisson interval given by a single observation of zero events

Channel	SR I	SR II	SR III	SR IV
eμ est.	21^{+8}_{-8}	$0.4^{+0.4}_{-0.4}$	$0.4^{+0.4}_{-0.4}$	$0.02^{+0.02}_{-0.02}$
eμ actual	24^{+12}_{-7}	$0.6^{+0.4}_{-0.3}$	$0.0^{+0.2}_{-0.0}$	$0.00^{+0.24}_{-0.00}$
ee est.	27^{+12}_{-12}	$0.7^{+0.4}_{-0.3}$	$0.6^{+0.4}_{-0.3}$	$0.02^{+0.01}_{-0.01}$
ee actual	22^{+7}_{-5}	$0.3^{+0.3}_{-0.1}$	$1.0^{+1.4}_{-0.7}$	$0.00^{+0.58}_{-0.00}$
$\mu\mu$ est.	4^{+2}_{-2}	$0.08^{+0.06}_{-0.06}$	$0.05^{+0.04}_{-0.04}$	$0.004^{+0.003}_{-0.003}$
$\mu\mu$ actual	10^{+7}_{-4}	$0.11^{+0.21}_{-0.07}$	$0.06^{+0.21}_{-0.06}$	$0.078^{+0.210}_{-0.078}$

ciency of cosmic ray muon events to survive the cosmic ray muon rejection criteria, which is found to be <0.03% from a dedicated data sample of cosmic ray muon events. With this study, we find a negligible number of cosmic ray muon events in data.

To estimate an upper limit on the amount of heavy-flavor background in the SR and to check that this background is covered within the nominal background prediction, several studies are performed. First, we perform the nominal ABCD method while additionally requiring at least one b-tagged jet, using the medium working point of the combined secondary vertices algorithm (version 2) [63]. In the $\mu\mu$ channel, which has the smallest relative SR contribution from mismeasurements and thus the most sensitivity to heavy-flavor backgrounds, we find that the estimate with at least one b-tagged jet is negligible. In the second study of the heavy-flavor background in the SR, we look at samples in which we invert the isolation criterion for events that pass the $\mu\mu$ preselection, for data and simulated background from muon-enriched QCD multijet events. These samples are dominated by muons from decays of b hadrons, and the QCD multijet simulation describes the data well in the region outside of the Z boson peak in the invariant mass distribution. We perform a naive ABCD estimate with the QCD multijet simulation and find no evidence for $|d_0|$ dependence, which indicates that the nominal background estimation already accounts for the heavy-flavor background. In the last heavy-flavor background study, we estimate this particular background in the SRs from the ratios of the number of events in each SR to the number of events in the prompt CR, from the QCD multijet simulation in the nonisolated region. We multiply these ratios by a normalization factor obtained from the number of QCD multijet simulated events that pass the nominal $\mu\mu$ preselection. Using this approach, we estimate that the heavy-flavor background is about 2 (20)% of the nominal background esti-

mate in SR I (IV), which is well covered within the nominal prediction uncertainties.

To investigate possible SR contributions from displaced leptonic decays of SM hadrons, we examine 2018 data and QCD multijet simulation in the $\mu\mu$ channel with both the muon isolation and ΔR requirements inverted. When the SR muon displacement criteria are applied, this region is dominated by events with dimuon invariant masses near those of the J/ψ and ψ(2S) mesons. Such events likely result from b hadron decays and are therefore already covered by the studies described in the previous paragraph, but we nevertheless estimate an upper bound on their SR contribution as an independent check. Using data in this inverted-isolation, inverted-ΔR region, we find the ratios of the number of events in each SR to the number of events in the prompt CR. We multiply these ratios by a normalization factor found from QCD multijet simulated events and find that the SM hadron contribution is less than 0.2% of the nominal prediction in SR I, which is negligible, and about 17% of the nominal prediction in SR IV, which is well covered by the large systematic uncertainty in this SR.

8 Systematic uncertainties in the signal efficiency

The systematic uncertainty in the background estimation method is the most significant one in the analysis: varying the nuisance parameter by one standard deviation shifts the best fit signal strength by about 5%. The following paragraphs describe the systematic uncertainties that are applied to the signal efficiency.

The integrated luminosities of the 2016, 2017, and 2018 data-taking periods are individually known with uncertainties in the 1.2–2.5% range [64–66], which when combined for the data set used in this analysis results in a total uncertainty of 1.8%, the improvement in precision reflecting the uncorrelated time evolution of some systematic effects.

The simulation of pileup events assumes a total inelastic pp cross section of 69.2 mb, with an associated uncertainty of 5% [67]. The systematic uncertainty arising as a result of the modeling of pileup events is estimated by varying the cross section of the minimum-bias events by 5% when generating the target pileup distributions. The pileup weights are recomputed with these new distributions and applied to the simulated events to obtain the variation in the yields in the inclusive SR. The average uncertainty is <1%. We treat these uncertainties as 100% correlated across the three years of data taking.

The trigger efficiency systematic uncertainty is given by the uncertainty in the measured trigger efficiency scale factors. These uncertainties are about 1% for the eμ and $\mu\mu$ channels and 10–19% for the ee channel. The uncertainty is larger for the ee channel relative to the other two channels

because there are fewer events available for the efficiency measurement in this channel. In addition, to cover the systematic variation observed in the muon trigger efficiency in signal simulation over the full $|d_0|$ range, we assign an additional 20% uncertainty. We treat these uncertainties as 100% correlated across the three data-taking years.

The efficiency to reconstruct displaced, isolated, high-p_T muons can be measured using cosmic ray muon events, as they also have these properties. The tracking efficiency of displaced muons is measured using cosmic ray muon events in simulation and data, and this efficiency is also used as a proxy for the tracking efficiency for displaced electrons. We take the difference in the mean efficiency between data and simulation as a systematic uncertainty in the signal yield. This uncertainty is 2–14%, depending on the data-taking year. The 2017 and 2018 systematic uncertainties are treated as fully correlated, while the 2016 uncertainty is treated as uncorrelated with the 2017 and 2018 uncertainties, since the pixel detector was upgraded after the 2016 data taking. The choice of how to correlate the uncertainties does not significantly affect the results.

One selection within the muon identification could have some dependence on $|d_0|$, namely, the requirement that the muons have at least one pixel detector hit. We find the efficiency of this criterion in simulated cosmic ray muon events and cosmic ray muon events from data, and we apply the difference in mean efficiency between data and simulation as a systematic uncertainty in the signal yield. The average uncertainty is about 16 (32)% in the eμ ($\mu\mu$) channel. The 2017 and 2018 systematic uncertainties are treated as fully correlated, while the 2016 uncertainty is treated as uncorrelated with the 2017 and 2018 uncertainties, since the pixel detector was upgraded after the 2016 data taking. Although we apply a similar pixel detector hit requirement on electrons, we do not apply a systematic uncertainty for electrons because it would require a sample of displaced electrons in data, which is difficult to obtain and verify. We checked that adding such a systematic uncertainty would not significantly affect the results.

For the two systematic uncertainties derived with cosmic ray muon events, the largest uncertainty is in 2016, compared with relatively smaller uncertainties in 2017 and 2018. This is in part because the 2016 cosmic data sample is much smaller, meaning that the statistical uncertainties are larger in this year. In addition, the uncertainty is reduced in 2017 and 2018 due to the upgrade of the pixel tracker, which allows for more precise tracking measurements.

To find the systematic uncertainty associated with the corrections to the lepton identification and isolation, we fluctuate the lepton scale factors up and down by their uncertainties and observe the change in the simulated event yields in the inclusive SR. The average uncertainty for electrons is about 3% in the eμ channel and about 7% in the ee channel, while

Table 5 Systematic uncertainties in the signal efficiency, for all three years and the three channels. For many sources of uncertainty, a range indicating the 68% confidence level of the spread is given. Uncertainties in the same row are treated as correlated among the data-taking years, except for the displaced tracking and pixel detector hit efficiencies for muons, where the 2016 uncertainty is treated as uncorrelated with the 2017 and 2018 uncertainties, as explained in the text

Systematic uncertainty	2016	2017	2018
Integrated luminosity			
All channels		1.8% (2016–2018)	
Pileup			
eμ channel	0.2–0.7%	0.4–0.9%	0.3–0.7%
ee channel	0.1–0.9%	0.5–1.2%	0.4–1.2%
$\mu\mu$ channel	0–0.4%	0–0.3%	0–0.4%
Trigger efficiency			
eμ channel, electrons	1.6%	1.3%	1.2%
eμ channel, muons	1.6%	1.4%	1.2%
ee channel	10%	13%	19%
$\mu\mu$ channel	1.2%	1.0%	1.1%
Muon trigger efficiency at large $|d_0|$			
eμ channel, muons	20%	20%	20%
$\mu\mu$ channel	20%	20%	20%
Displaced tracking efficiency			
All channels	14%	5.8%	2.4%
Pixel detector hit efficiency for muons			
eμ channel, muons	30–32%	10–13%	12–17%
$\mu\mu$ channel	70–74%	20–24%	27–31%
Lepton identification and isolation			
eμ channel, electrons	1.2–1.3%	3.1–4.0%	3.1–3.9%
eμ channel, muons	0.04–0.05%	0.06–0.07%	0.05–0.06%
ee channel	2.3–2.5%	6.4–7.9%	6.3–7.7%
$\mu\mu$ channel	0.09–0.10%	0.14–0.15%	0.11–0.13%

the average uncertainty for muons is <1%. We treat these uncertainties as 100% correlated across the three data-taking years.

To find the systematic uncertainty associated with the corrections to the lepton $|d_0|$, we fluctuate the lepton $|d_0|$ corrections up and down by their uncertainties and observe the change in the simulated event yields in the inclusive SR. We find that this uncertainty is negligible in 2017 and 2018, and there is no $|d_0|$ correction needed for the 2016 simulation.

The systematic uncertainties in the signal efficiency are summarized in Table 5.

9 Results

Figure 3 shows the expected number of background events and the observed data, with a representative signal overlaid, in each p_T bin and each SR, for each channel. Because the electron $|d_0|$ values are measured less precisely than those of muons, the background estimates are generally greatest in the ee channel, despite its stricter p_T requirements. Furthermore, the 2016 data contributes relatively more background events than the 2017–2018 data because of the improved $|d_0|$ resolution after the pixel detector upgrade. We also note that

the background predictions are lowest in SR IV, especially when there is at least one muon in the final state.

The observed number of events is consistent with the predicted amount of background. All data points are observed to deviate by less than ±2 standard deviations from the expected standard model background, for each analysis channel as well as for the channel combination.

In the high-p_T SR I bin, which is the most sensitive bin for large top squark masses and small $c\tau_0$ values, particularly $c\tau_0 \lesssim 1$ cm, the eμ channel has the largest signal yield relative to the other two channels. As described above, this is because there are twice as many chances to have one electron and one muon, since the top squarks decay to each lepton flavor with equal probability. In this bin, the ee and $\mu\mu$ channel signal yields are similar. In SR IV, which is the most sensitive bin for large top squark masses and long lifetimes, the $\mu\mu$ channel has the largest signal yield for $c\tau_0 \gtrsim 10$ cm, relative to the other two channels. This is because the muon reconstruction and selection efficiency is better than that of electrons, which is particularly true at large $|d_0|$ values. In this bin, the eμ and $\mu\mu$ channels have similar amounts of background, and the ee channel has the smallest signal yield out of the three channels for $c\tau_0 \gtrsim 10$ cm. Therefore, for large top squark masses, the eμ channel is the most sensitive
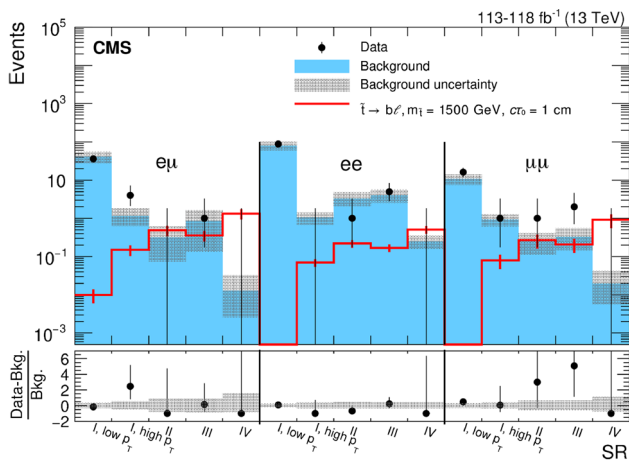
Fig. 3 The number of observed and estimated background events in each channel and SR, with a representative signal overlaid. The lower panel shows the fractional difference between the data and the background. For each background estimate and signal yield, the total uncertainty (statistical plus systematic) is given. For each observed yield, the 68% Poisson confidence interval is given. The distributions shown are those obtained before the final maximum likelihood fit to the data

for $c\tau_0 \lesssim 10$ cm and the $\mu\mu$ (ee) channel is the most (least) sensitive for $c\tau_0 \gtrsim 10$ cm. For a given $c\tau_0$ and mass, the relative distribution of signal events across SRs is similar for all benchmark signals we consider.

We perform a simultaneous counting experiment in each SR bin for most of the interpretations we consider. However, the ee and $\mu\mu$ channels are fit individually to calculate limits on GMSB models with a $\tilde{e}$ or $\tilde{\mu}$ NLSP. We set 95% confidence level (CL) upper limits on the product of the signal production cross section and branching fraction to leptons ($\sigma\mathcal{B}$), using a modified frequentist method [68–72]. This approach uses the profile likelihood ratio determined by pseudo-experiments as the test statistic [71] and the CL_s criterion. The expected and observed upper limits are evaluated through the use of pseudodata sets. Potential signal contributions to event counts in the SRs and CRs are taken into consideration, as are correlated statistical uncertainties that arise when CR event counts are used to predict the number of background events in multiple SRs. The systematic uncertainties and their correlations are incorporated in the likelihood as nuisance parameters with log-normal probability density functions. The statistical uncertainties in the signal and background estimates are modeled with gamma functions. By comparing the expected and observed cross section limits to the theoretical cross sections at NLO, mass and $c\tau_0$ exclusion limits are set for each of the models we consider.

Figures 4, 5, and 6 show the limits for the top squarks, sleptons, and exotic Higgs bosons, respectively. The top squark limits assume either $\mathcal{B}(\tilde{t} \to d\ell)$ or $\mathcal{B}(\tilde{t} \to b\ell)$ is 100%, and each lepton has an equal probability of being an electron, a muon, or a tau lepton. The slepton limits assume that the

superpartners of the left- and right-handed leptons are degenerate in mass. The Higgs boson limits assume that the mass of S is 30 or 50 GeV, $\mathcal{B}(\text{H} \to \text{SS}) = 100\%$, and each S has a 50% probability of decaying to two electrons or two muons. The S masses are chosen as two kinematically accessible benchmark values. In Figs. 4 and 5, the area to the left of the solid curves represents the observed exclusion region, and the dashed lines indicate the expected limits. The maximum sensitivity of this search occurs at $c\tau_0 = 2$ cm, where $\tilde{t}$ masses up to 1500 GeV are excluded. The sensitivity degrades for $\tilde{t}$ masses and $c\tau_0$ values above and below this point. The previous CMS analysis [26], which was performed only in the $e\mu$ channel and at $\sqrt{s} = 8$ TeV, excluded $\tilde{t}$ masses up to 790 GeV at a $c\tau_0$ of 2 cm. As a result of the higher $\sqrt{s}$ and integrated luminosity, as well as the addition of the same-flavor channels, the mass exclusion limits for this search improve upon the previous CMS analysis by approximately a factor of 2. Furthermore, this search can be directly compared with the search described in Ref. [16], which looks for displaced leptons with the ATLAS detector at $\sqrt{s} = 13$ TeV. The smaller $|d_0|$ lower bound of the SRs enables the present analysis to have greater sensitivity to shorter slepton lifetimes than the ATLAS analysis.

10 Summary

A search has been presented for long-lived particles decaying to displaced leptons in proton–proton collisions at $\sqrt{s} = 13$ TeV at the LHC. With collision data recorded in 2016, 2017, and 2018, and corresponding to an integrated luminosity of 113–118 fb^{-1}, no excess above the estimated background has been observed. Exclusion limits have been set at 95% confidence level. Top squarks with masses between 100 and at least 460 GeV have been excluded for $0.01 < c\tau_0 < 1000$ cm, with a maximum exclusion of 1500 GeV occurring at $c\tau_0 = 2$ cm, where $c\tau_0$ is the proper decay length. These exclusions assume that 100% of the top squarks decay to a lepton and a d or b quark, where the lepton has an equal probability of being an electron, muon, or tau lepton. The following exclusions assume that the superpartners of the left- and right-handed leptons are mass degenerate. Electron superpartners with masses of at least 50 GeV have been excluded for $0.007 < c\tau_0 < 70$ cm, with a maximum exclusion of 610 GeV occurring at $c\tau_0 = 0.7$ cm. Muon superpartners with masses of at least 50 GeV have been excluded for $0.005 < c\tau_0 < 265$ cm, with a maximum exclusion of 610 GeV occurring at $c\tau_0 = 3$ cm. Tau lepton superpartners with masses of at least 50 GeV have been excluded for $0.015 < c\tau_0 < 20$ cm, with a maximum exclusion of 405 GeV occurring at $c\tau_0 = 2$ cm. In the case that electron, muon, and tau lepton superpartners are mass degenerate, lepton superpartners with masses between 50 and at least
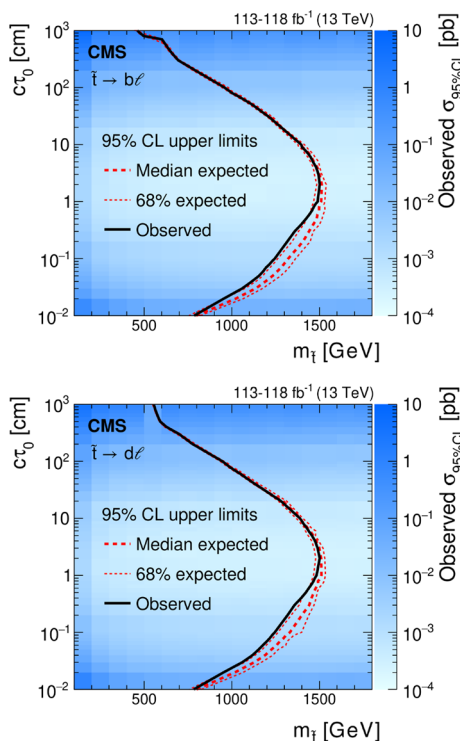
Fig. 4 The observed 95% CL upper limits on the long-lived top squark production cross section, in the $c\tau_0$-mass plane, for the three channels combined. The $\tilde{t} \to b\ell$ (upper) and $\tilde{t} \to d\ell$ (lower) processes are shown. These limits assume either $\mathcal{B}(\tilde{t} \to d\ell)$ or $\mathcal{B}(\tilde{t} \to b\ell)$ is 100%, and each lepton has an equal probability of being an electron, a muon, or a tau lepton. The area to the left of the black curve represents the observed exclusion region, and the dashed red lines indicate the expected limits and their 68% confidence intervals
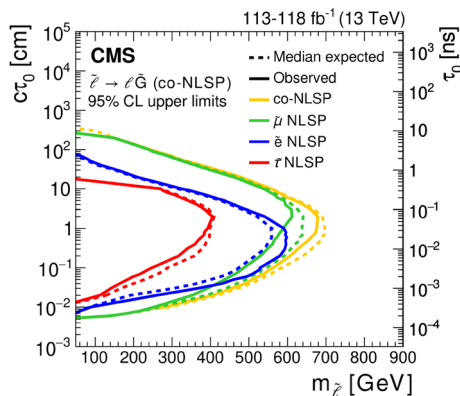
Fig. 5 The 95% CL constraints on the long-lived slepton $c\tau_0$ and mass. The $\tilde{\tau}$ and co-NLSP limits are shown for the three channels combined, while the $\tilde{e}$ and $\tilde{\mu}$ NLSP limits are shown for the ee and $\mu\mu$ channels, respectively. These limits assume that the superpartners of the left- and right-handed leptons are degenerate in mass and $\mathcal{B}(\tilde{\ell} \to \ell\tilde{G})$ is 100%. The area to the left of the solid curves represents the observed exclusion region, and the dashed lines indicate the expected limits

Fig. 6 The 95% CL upper limits on the H $\to$ SS, S $\to$ $\ell^+\ell^-$ branching fraction as a function of $c\tau_0$, for a Higgs boson with a mass of 125 GeV and a long-lived scalar with a mass of 30 GeV or 50 GeV, for the three channels combined. These limits assume that $\mathcal{B}(H \to SS) = 100\%$ and each S has a 50% probability of decaying to two electrons or two muons. The area above the solid (dashed) curve represents the observed (expected) exclusion region

sensitive results published to date. For $0.10 < c\tau_0 < 12$ cm, branching fractions greater than 0.03% have been excluded for 125 GeV Higgs bosons decaying to two long-lived scalar particles, assuming each has a mass of 30 GeV and decays with equal probability to electrons or muons. For scalar particles with $0.1 < c\tau_0 < 1000$ cm that decay to any final state, these are the most sensitive results published to date.

270 GeV have been excluded for $0.005 < c\tau_0 < 265$ cm, with a maximum exclusion of 680 GeV occurring at $c\tau_0 = 2$ cm. For sleptons with $c\tau_0 < 0.8$ cm, these are the most

Declaration

References

1. ATLAS Collaboration, Search for magnetic monopoles and stable high-electric-charge objects in 13 TeV proton–proton collisions with the ATLAS detector. Phys. Rev. Lett. **124**, 031802 (2020). https://doi.org/10.1103/PhysRevLett.124.031802 arXiv:1905.10130

2. ATLAS Collaboration, Search for heavy charged long-lived particles in the ATLAS detector in 36.1 fb^{-1} of proton–proton collision data at $\sqrt{s}$ = 13 TeV. Phys. Rev. D **99**, 092007 (2019). https://doi.org/10.1103/PhysRevD.99.092007 arXiv:1902.01636

3. CMS Collaboration, Search for disappearing tracks in proton–proton collisions at $\sqrt{s}$ = 13 TeV. Phys. Lett. B **806**, 135502 (2020). https://doi.org/10.1016/j.physletb.2020.135502 arXiv:2004.05153

4. CMS Collaboration, Searches for physics beyond the standard model with the M_{T2} variable in hadronic final states with and without disappearing tracks in proton-proton collisions at $\sqrt{s}$ = 13 TeV. Eur. Phys. J. C **80**, 3 (2020). https://doi.org/10.1140/epjc/s10052-019-7493-x arXiv:1909.03460

5. ATLAS Collaboration, Search for long-lived charginos based on a disappearing-track signature in pp collisions at $\sqrt{s}$ = 13 TeV with the ATLAS detector. JHEP **06**, 022 (2018). https://doi.org/10.1007/JHEP06(2018)022 arXiv:1712.02118

6. CMS Collaboration, Search for long-lived particles using displaced jets in proton–proton collisions at $\sqrt{s}$ = 13 TeV. Phys. Rev. D **104**, 012015 (2021). https://doi.org/10.1103/PhysRevD.104.012015 arXiv:2012.01581

7. CMS Collaboration, Search for long-lived particles using nonprompt jets and missing transverse momentum with proton–proton collisions at $\sqrt{s}$ = 13 TeV. Phys. Lett. B **797**, 134876 (2019). https://doi.org/10.1016/j.physletb.2019.134876 arXiv:1906.06441

8. ATLAS Collaboration, Search for long-lived neutral particles in pp collisions at $\sqrt{s}$ = 13 TeV that decay into displaced hadronic jets in the ATLAS calorimeter. Eur. Phys. J. C **79**, 481 (2019). https://doi.org/10.1140/epjc/s10052-019-6962-6 arXiv:1902.03094

9. ATLAS Collaboration, Search for long-lived particles produced in pp collisions at $\sqrt{s}$ = 13 TeV that decay into displaced hadronic jets in the ATLAS muon spectrometer. Phys. Rev. D **99**, 052005 (2019). https://doi.org/10.1103/PhysRevD.99.052005 arXiv:1811.07370

10. ATLAS Collaboration, Search for long-lived neutral particles produced in pp collisions at $\sqrt{s}$ = 13 TeV decaying into displaced hadronic jets in the ATLAS inner detector and muon spectrometer. Phys. Rev. D **101**, 052013 (2020). https://doi.org/10.1103/PhysRevD.101.052013 arXiv:1911.12575

11. LHCb Collaboration, Updated search for long-lived particles decaying to jet pairs. Eur. Phys. J. C **77**, 812 (2017). https://doi.org/10.1140/epjc/s10052-017-5178-x arXiv:1705.07332

12. LHCb Collaboration, Search for Higgs-like bosons decaying into long-lived exotic particles. Eur. Phys. J. C **76**, 664 (2016). https://doi.org/10.1140/epjc/s10052-016-4489-7 arXiv:1609.03124

13. CMS Collaboration, Search for long-lived particles using delayed photons in proton–proton collisions at $\sqrt{s}$ = 13 TeV. Phys. Rev. D **100**, 112003 (2019). https://doi.org/10.1103/PhysRevD.100.112003 arXiv:1909.06166

14. ATLAS Collaboration, Search for nonpointing and delayed photons in the diphoton and missing transverse momentum final state in 8 TeV pp collisions at the LHC using the ATLAS detector. Phys. Rev. D **90**, 112005 (2014). https://doi.org/10.1103/PhysRevD.90.112005 arXiv:1409.5542

15. CMS Collaboration, Search for long-lived particles that decay into final states containing two electrons or two muons in proton-proton collisions at $\sqrt{s}$ = 8 TeV. Phys. Rev. D **91**, 052012 (2015). https://doi.org/10.1103/PhysRevD.91.052012 arXiv:1411.6977

16. ATLAS Collaboration, Search for displaced leptons in $\sqrt{s}$ = 13 TeV pp collisions with the ATLAS detector. Phys. Rev. Lett. **127**, 051802 (2021). https://doi.org/10.1103/PhysRevLett.127.051802 arXiv:2011.07812

17. ATLAS Collaboration, Search for heavy neutral leptons in decays of W bosons produced in 13 TeV pp collisions using prompt and displaced signatures with the ATLAS detector. JHEP **10**, 265 (2019). https://doi.org/10.1007/JHEP10(2019)265 arXiv:1905.09787

18. ATLAS Collaboration, Search for long-lived, massive particles in events with a displaced vertex and a muon with large impact parameter in pp collisions at $\sqrt{s}$ = 13 TeV with the ATLAS detector. Phys. Rev. D **102**, 032006 (2020). https://doi.org/10.1103/PhysRevD.102.032006 arXiv:2003.11956

19. ATLAS Collaboration, Search for displaced vertices of oppositely charged leptons from decays of long-lived particles in pp collisions at $\sqrt{s}$ =13 TeV with the ATLAS detector. Phys. Lett. B **801**, 135114 (2020). https://doi.org/10.1016/j.physletb.2019.135114 arXiv:1907.10037

20. LHCb Collaboration, Search for long-lived particles decaying to $e^{\pm}\mu^{\mp}\nu$. Eur. Phys. J. C **81**, 261 (2021). https://doi.org/10.1140/epjc/s10052-021-08994-0 arXiv:2012.02696

21. LHCb Collaboration, Search for long-lived scalar particles in $B^+ \rightarrow K^+\chi(\mu^+\mu^-)$ decays. Phys. Rev. D **95**, 071101 (2017). https://doi.org/10.1103/PhysRevD.95.071101 arXiv:1612.07818

22. CMS Collaboration, Search for decays of stopped exotic long-lived particles produced in proton–proton collisions at $\sqrt{s}$ = 13 TeV. JHEP **05**, 127 (2018). https://doi.org/10.1007/JHEP05(2018)127 arXiv:1801.00359

23. ATLAS Collaboration, A search for the decays of stopped long-lived particles at $\sqrt{s}$ = 13 TeV with the ATLAS detector. JHEP **07**, 173 (2021). https://doi.org/10.1007/JHEP07(2021)173 arXiv:2104.03050

24. ATLAS Collaboration, Search for light long-lived neutral particles produced in pp collisions at $\sqrt{s}$ = 13 TeV and decaying into collimated leptons or light hadrons with the ATLAS detector. Eur. Phys. J. C **80**, 450 (2020). https://doi.org/10.1140/epjc/s10052-020-7997-4 arXiv:1909.01246

25. LHCb Collaboration, Search for massive long-lived particles decaying semileptonically at $\sqrt(s)$ = 13 TeV (2021). arXiv:2110.07293 (**Submitted to Eur. Phys. J. C**)

26. CMS Collaboration, Search for displaced supersymmetry in events with an electron and a muon with large impact parameters. Phys. Rev. Lett. **114**, 061801 (2015). https://doi.org/10.1103/PhysRevLett.114.061801 arXiv:1409.4789

27. P. Graham, D. Kaplan, S. Rajendran, P. Sarawat, Displaced supersymmetry. JHEP **07**, 149 (2012). https://doi.org/10.1007/JHEP07(2012)149 arXiv:1204.6038

28. R. Barbier et al., *R*-parity-violating supersymmetry. Phys. Rep. **420**, 1 (2005). https://doi.org/10.1016/j.physrep.2005.08.006 arXiv:hep-ph/0406039

29. J.A. Evans, J. Shelton, Long-lived status and displaced leptons at the LHC. JHEP **04**, 056 (2016). https://doi.org/10.1007/JHEP04(2016)056 arXiv:1601.01326

30. M.J. Strassler, K.M. Zurek, Discovering the Higgs through highly-displaced vertices. Phys. Lett. B **661**, 263 (2008). https://doi.org/10.1016/j.physletb.2008.02.008 arXiv:hep-ph/0605193

31. HEPData record for this analysis (2021). https://doi.org/10.17182/hepdata.113658

32. CMS Tracker Group Collaboration, The CMS Phase-1 pixel detector upgrade. JINST **16**, P02027 (2021). https://doi.org/10.1088/1748-0221/16/02/P02027 arXiv:2012.14304

33. CMS Collaboration, Track impact parameter resolution for the full pseudorapidity coverage in the 2017 dataset with the CMS Phase-1 pixel detector. CMS Detector Performance Summary CMS-DP-2020-049 (2020) http://cds.cern.ch/record/2743740

34. CMS Collaboration, Description and performance of track and primary-vertex reconstruction with the CMS tracker. JINST **9**, P10009 (2014). https://doi.org/10.1088/1748-0221/9/10/P10009 arXiv:1405.6569

35. CMS Collaboration, Performance of the CMS Level-1 trigger in proton–proton collisions at $\sqrt{s}$ = 13 TeV. JINST **15**, P10017 (2020). https://doi.org/10.1088/1748-0221/15/10/P10017 arXiv:2006.10165

36. CMS Collaboration, The CMS trigger system. JINST **12**, P01020 (2017). https://doi.org/10.1088/1748-0221/12/01/P01020 arXiv:1609.02366

37. CMS Collaboration, Performance of the CMS muon trigger system in proton-proton collisions at $\sqrt{s}$ = 13 TeV. JINST **16**, P07001 (2021). https://doi.org/10.1088/1748-0221/16/07/P07001 arXiv:2102.04790

38. CMS Collaboration, The CMS experiment at the CERN LHC. JINST **3**, S08004 (2008). https://doi.org/10.1088/1748-0221/3/08/S08004

39. NNPDF Collaboration, Parton distributions for the LHC Run II. JHEP **04**, 040 (2015). https://doi.org/10.1007/JHEP04(2015)040 arXiv:1410.8849

40. NNPDF Collaboration, Parton distributions from high-precision collider data. Eur. Phys. J. C **77**, 663 (2017). https://doi.org/10.1140/epjc/s10052-017-5199-5 arXiv:1706.00428

41. T. Sjöstrand et al., An introduction to PYTHIA 8.2. Comput. Phys. Commun. **191**, 159 (2015). https://doi.org/10.1016/j.cpc.2015.01.024 arXiv:1410.3012

42. CMS Collaboration, Event generator tunes obtained from underlying event and multiparton scattering measurements. Eur. Phys. J. C **76**, 155 (2016). https://doi.org/10.1140/epjc/s10052-016-3988-x arXiv:1512.00815

43. CMS Collaboration, Extraction and validation of a new set of CMS PYTHIA8 tunes from underlying-event measurements. Eur. Phys. J. C **80**, 4 (2020). https://doi.org/10.1140/epjc/s10052-019-7499-4 arXiv:1903.12179

44. GEANT4 Collaboration, Geant4: a simulation toolkit. Nucl. Instrum. Methods A **506**, 250 (2003). https://doi.org/10.1016/S0168-9002(03)01368-8

45. J. Alwall et al., The automated computation of tree-level and next-to-leading order differential cross sections, and their matching to parton shower simulations. JHEP **07**, 079 (2014). https://doi.org/10.1007/JHEP07(2014)079 arXiv:1405.0301

46. J. Alwall et al., Comparative study of various algorithms for the merging of parton showers and matrix elements in hadronic collisions. Eur. Phys. J. C **53**, 473 (2008). https://doi.org/10.1140/epjc/s10052-007-0490-5 arXiv:0706.2569

47. S. Frixione, B.R. Webber, Matching NLO QCD computations and parton shower simulations. JHEP **06**, 029 (2002). https://doi.org/10.1088/1126-6708/2002/06/029 arXiv:hep-ph/0204244

48. P. Nason, A new method for combining NLO QCD with shower Monte Carlo algorithms. JHEP **11**, 040 (2004). https://doi.org/10.1088/1126-6708/2004/11/040 arXiv:hep-ph/0409146

49. S. Frixione, P. Nason, C. Oleari, Matching NLO QCD computations with parton shower simulations: the POWHEG method. JHEP **11**, 070 (2007). https://doi.org/10.1088/1126-6708/2007/11/070 arXiv:0709.2092

50. S. Alioli, P. Nason, C. Oleari, E. Re, NLO vector-boson production matched with shower in POWHEG. JHEP **07**, 060 (2008). https://doi.org/10.1088/1126-6708/2008/07/060 arXiv:0805.4802

51. S. Alioli, P. Nason, C. Oleari, E. Re, A general framework for implementing NLO calculations in shower Monte Carlo programs: the POWHEG BOX. JHEP **06**, 043 (2010). https://doi.org/10.1007/JHEP06(2010)043 arXiv:1002.2581

52. R. Mackeprang, A. Rizzi, Interactions of coloured heavy stable particles in matter. Eur. Phys. J. C **50**, 353 (2007). https://doi.org/10.1140/epjc/s10052-007-0252-4 arXiv:hep-ph/0612161

53. R. Mackeprang, D. Milstead, An updated description of heavy-hadron interactions in Geant4. Eur. Phys. J. C **66**, 493 (2010). https://doi.org/10.1140/epjc/s10052-010-1262-1 arXiv:0908.1868

54. CMS Collaboration, Performance of electron reconstruction and selection with the CMS detector in proton–proton collisions at $\sqrt{s} = 8$ TeV. JINST **10**, P06005 (2015). https://doi.org/10.1088/1748-0221/10/06/P06005 arXiv:1502.02701

55. CMS Collaboration, Electron and photon reconstruction and identification with the CMS experiment at the CERN LHC. JINST **16**, P05014 (2021). https://doi.org/10.1088/1748-0221/16/05/P05014 arXiv:2012.06888

56. CMS Collaboration, Performance of the CMS muon detector and muon reconstruction with proton–proton collisions at $\sqrt{s} = 13$ TeV. JINST **13**, P06015 (2018). https://doi.org/10.1088/1748-0221/13/06/P06015 arXiv:1804.04528

57. CMS Collaboration, Particle-flow reconstruction and global event description with the CMS detector. JINST **12**, P10003 (2017). https://doi.org/10.1088/1748-0221/12/10/P10003 arXiv:1706.04965

58. M. Cacciari, G.P. Salam, G. Soyez, The anti-k_T jet clustering algorithm. JHEP **04**, 063 (2008). https://doi.org/10.1088/1126-6708/2008/04/063 arXiv:0802.1189

59. M. Cacciari, G.P. Salam, G. Soyez, FastJet user manual. Eur. Phys. J. C **72**, 1896 (2012). https://doi.org/10.1140/epjc/s10052-012-1896-2 arXiv:1111.6097

60. CMS Collaboration, Precision measurement of the structure of the CMS inner tracking system using nuclear interactions. JINST **13**, P10034 (2018). https://doi.org/10.1088/1748-0221/13/10/P10034 arXiv:1807.03289

61. R. Frühwirth, Application of Kalman filtering to track and vertex fitting. Nucl. Instrum. Methods A **262**, 444 (1987). https://doi.org/10.1016/0168-9002(87)90887-4

62. R. Frühwirth, P. Kubinec, W. Mitaroff, M. Regler, Vertex reconstruction and track bundling at the LEP collider using robust algorithms. Comput. Phys. Commun. **96**, 189 (1996). https://doi.org/10.1016/0010-4655(96)00040-9

63. CMS Collaboration, Identification of heavy-flavour jets with the CMS detector in pp collisions at 13 TeV. JINST **13**, P05011 (2018). https://doi.org/10.1088/1748-0221/13/05/P05011 arXiv:1712.07158

64. CMS Collaboration, Precision luminosity measurement in proton–proton collisions at $\sqrt{s} = 13$ TeV in 2015 and 2016 at CMS. Eur. Phys. J. C **81**, 800 (2021). https://doi.org/10.1140/epjc/s10052-021-09538-2 arXiv:2104.01927

65. CMS Collaboration, CMS luminosity measurements for the 2017 data-taking period at $\sqrt{s} = 13$ TeV. CMS Physics Analysis Summary CMS-PAS-LUM-17-004 (2018). http://cds.cern.ch/record/2621960

66. CMS Collaboration, CMS luminosity measurements for the 2018 data-taking period at $\sqrt{s} = 13$ TeV. CMS Physics Analysis Summary CMS-PAS-LUM-18-002 (2018). http://cds.cern.ch/record/2676164

67. CMS Collaboration, Measurement of the inelastic proton–proton cross section at $\sqrt{s} = 13$ TeV. JHEP **07**, 161 (2018). https://doi.org/10.1007/JHEP07(2018)161 arXiv:1802.02613

68. T. Junk, Confidence level computation for combining searches with small statistics. Nucl. Instrum. Methods A **434**, 435 (1999). https://doi.org/10.1016/S0168-9002(99)00498-2 arXiv:hep-ex/9902006

69. A.L. Read, Presentation of search results: the CL_s technique. J. Phys. G **28**, 2693 (2002). https://doi.org/10.1088/0954-3899/28/10/313

70. G. Cowan, K. Cranmer, E. Gross, O. Vitells, Asymptotic formulae for likelihood-based tests of new physics. Eur. Phys. J. C **71**, 1554 (2011). https://doi.org/10.1140/epjc/s10052-011-1554-0 arXiv:1007.1727 (**Erratum:** https://doi.org/10.1140/epjc/s10052-013-2501-z)

71. ATLAS and CMS Collaborations, and LHC Higgs Combination Group, Procedure for the LHC Higgs boson search combination in Summer 2011. Technical Report CMS-NOTE-2011-005, ATL-PHYS-PUB-2011-11 (2011). https://cds.cern.ch/record/1379837

72. R.D. Cousins, V.L. Highland, Incorporating systematic uncertainties into an upper limit. Nucl. Instrum. Methods A **320**, 331 (1992). https://doi.org/10.1016/0168-9002(92)90794-5

CMS Collaboration

Yerevan Physics Institute, Yerevan, Armenia
A. Tumasyan

Institut für Hochenergiephysik, Vienna, Austria
W. Adam, J. W. Andrejkovic, T. Bergauer, S. Chatterjee, K. Damanakis, M. Dragicevic, A. Escalante Del Valle, R. Frühwirth[1], M. Jeitler[1], N. Krammer, L. Lechner, D. Liko, I. Mikulec, P. Paulitsch, F. M. Pitters, J. Schieck[1], R. Schöfbeck, D. Schwarz, S. Templ, W. Waltenberger, C.-E. Wulz[1]
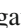
Institute for Nuclear Problems, Minsk, Belarus
V. Chekhovsky, A. Litomin, V. Makarenko

Universiteit Antwerpen, Antwerpen, Belgium
M. R. Darwish[2], E. A. De Wolf, T. Janssen, T. Kello[3], A. Lelek, H. Rejeb Sfar, P. Van Mechelen, S. Van Putte, N. Van Remortel

Vrije Universiteit Brussel, Brussel, Belgium
F. Blekman, E. S. Bols, J. D'Hondt, M. Delcourt, H. El Faham, S. Lowette, S. Moortgat, A. Morton, D. Müller, A. R. Sahasransu, S. Tavernier, W. Van Doninck

Université Libre de Bruxelles, Bruxelles, Belgium
D. Beghin, B. Bilin, B. Clerbaux, G. De Lentdecker, L. Favart, A. Grebenyuk, A. K. Kalsi, K. Lee, M. Mahdavikhorrami, I. Makarenko, L. Moureaux, L. Pétré, A. Popov, N. Postiau, E. Starling, L. Thomas, M. Vanden Bemden, C. Vander Velde, P. Vanlaer

Ghent University, Ghent, Belgium
T. Cornelis, D. Dobur, J. Knolle, L. Lambrecht, G. Mestdach, M. Niedziela, C. Roskas, A. Samalan, K. Skovpen, M. Tytgat, B. Vermassen, L. Wezenbeek
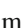
Université Catholique de Louvain, Louvain-la-Neuve, Belgium
A. Benecke, A. Bethani, G. Bruno, F. Bury, C. Caputo, P. David, C. Delaere, I. S. Donertas, A. Giammanco, K. Jaffel, Sa. Jain, V. Lemaitre, K. Mondal, J. Prisciandaro, A. Taliercio, M. Teklishyn, T. T. Tran, P. Vischia, S. Wertz

Centro Brasileiro de Pesquisas Fisicas, Rio de Janeiro, Brazil
G. A. Alves, C. Hensel, A. Moraes

Universidade do Estado do Rio de Janeiro, Rio de Janeiro, Brazil
W. L. Aldá Júnior, M. Alves Gallo Pereira, M. Barroso Ferreira Filho, H. Brandao Malbouisson, W. Carvalho, J. Chinellato[4], E. M. Da Costa, G. G. Da Silveira[5], D. De Jesus Damiao, S. Fonseca De Souza, C. Mora Herrera, K. Mota Amarilo, L. Mundim, H. Nogima, P. Rebello Teles, A. Santoro, S. M. Silva Do Amaral, A. Sznajder, M. Thiel, F. Torres Da Silva De Araujo[6], A. Vilela Pereira

Universidade Estadual Paulista[a], Universidade Federal do ABC[b], São Paulo, Brazil
C. A. Bernardes[a,5], L. Calligaris[a], T. R. Fernandez Perez Tomei[a], E. M. Gregores[a,b], D. S. Lemos[a], P. G. Mercadante[a,b], S. F. Novaes[a], Sandra S. Padula[a]

Institute for Nuclear Research and Nuclear Energy, Bulgarian Academy of Sciences, Sofia, Bulgaria
A. Aleksandrov, G. Antchev, R. Hadjiiska, P. Iaydjiev, M. Misheva, M. Rodozov, M. Shopova, G. Sultanov

University of Sofia, Sofia, Bulgaria
A. Dimitrov, T. Ivanov, L. Litov, B. Pavlov, P. Petkov, A. Petrov

Beihang University, Beijing, China
T. Cheng, T. Javaid[7], M. Mittal, L. Yuan

Department of Physics, Tsinghua University, Beijing, China
M. Ahmad, G. Bauer, C. Dozen[8], Z. Hu, J. Martins[9], Y. Wang, K. Yi[10,11]

Institute of High Energy Physics, Beijing, China
E. Chapon , G. M. Chen [7], H. S. Chen [7], M. Chen , F. Iemmi, A. Kapoor , D. Leggat, H. Liao, Z.-A. Liu [7],
V. Milosevic , F. Monti, R. Sharma , J. Tao , J. Thomas-wilsker, J. Wang, H. Zhang, J. Zhao

State Key Laboratory of Nuclear Physics and Technology, Peking University, Beijing, China
A. Agapitos, Y. An, Y. Ban, C. Chen, A. Levin , Q. Li , X. Lyu, Y. Mao, S. J. Qian, D. Wang , J. Xiao

Sun Yat-Sen University, Guangzhou, China
M. Lu, Z. You

Institute of Modern Physics and Key Laboratory of Nuclear Physics and Ion-beam Application (MOE)-Fudan University, Shanghai, China
X. Gao [3], H. Okawa, Y. Zhang

Zhejiang University, Hangzhou, China
Z. Lin, M. Xiao

Universidad de Los Andes, Bogota, Colombia
C. Avila , A. Cabrera, C. Florez , J. Fraga

Universidad de Antioquia, Medellin, Colombia
J. Mejia Guisao, F. Ramirez, J. D. Ruiz Alvarez , C. A. Salazar González

University of Split, Faculty of Electrical Engineering, Mechanical Engineering and Naval Architecture, Split, Croatia
D. Giljanovic, N. Godinovic , D. Lelas, I. Puljak

University of Split, Faculty of Science, Split, Croatia
Z. Antunovic, M. Kovac, T. Sculac

Institute Rudjer Boskovic, Zagreb, Croatia
V. Brigljevic , D. Ferencek , D. Majumder , M. Roguljic, A. Starodumov [12], T. Susa

University of Cyprus, Nicosia, Cyprus
A. Attikis, K. Christoforou, E. Erodotou, A. Ioannou, G. Kole , M. Kolosova, S. Konstantinou, J. Mousa , C. Nicolaou,
F. Ptochos , P. A. Razis, H. Rykaczewski, H. Saka

Charles University, Prague, Czech Republic
M. Finger [13], M. Finger Jr. [13], A. Kveton

Escuela Politecnica Nacional, Quito, Ecuador
E. Ayala

Universidad San Francisco de Quito, Quito, Ecuador
E. Carrera Jarrin

Academy of Scientific Research and Technology of the Arab Republic of Egypt, Egyptian Network of High Energy Physics, Cairo, Egypt
H. Abdalla [14], Y. Assran [15,16]

Center for High Energy Physics (CHEP-FU), Fayoum University, El-Fayoum, Egypt
A. Lotfy, M. A. Mahmoud

National Institute of Chemical Physics and Biophysics, Tallinn, Estonia
S. Bhowmik , R. K. Dewanjee , K. Ehataht, M. Kadastik, S. Nandan, C. Nielsen, J. Pata, M. Raidal , L. Tani,
C. Veelken
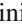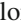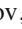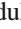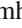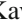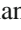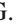
Department of Physics, University of Helsinki, Helsinki, Finland
P. Eerola , L. Forthomme , H. Kirschenmann , K. Osterberg, M. Voutilainen

Helsinki Institute of Physics, Helsinki, Finland
S. Bharthuar, E. Brücken, F. Garcia, J. Havukainen, M. S. Kim, R. Kinnunen, T. Lampén, K. Lassila-Perini, S. Lehti,
T. Lindén, M. Lotti, L. Martikainen, M. Myllymäki, J. Ott, H. Siikonen, E. Tuominen , J. Tuominiemi

Lappeenranta University of Technology, Lappeenranta, Finland

P. Luukka, H. Petrow, T. Tuuva

IRFU, CEA, Université Paris-Saclay, Gif-sur-Yvette, France

C. Amendola, M. Besancon, F. Couderc, M. Dejardin, D. Denegri, J. L. Faure, F. Ferri, S. Ganjour, P. Gras, G. Hamel de Monchenault, P. Jarry, B. Lenzi, E. Locci, J. Malcles, J. Rander, A. Rosowsky, M. Ö. Sahin, A. Savoy-Navarro[17], M. Titov, G. B. Yu

Laboratoire Leprince-Ringuet, CNRS/IN2P3, Ecole Polytechnique, Institut Polytechnique de Paris, Palaiseau, France

S. Ahuja, F. Beaudette, M. Bonanomi, A. Buchot Perraguin, P. Busson, A. Cappati, C. Charlot, O. Davignon, B. Diab, G. Falmagne, S. Ghosh, R. Granier de Cassagnac, A. Hakimi, I. Kucher, J. Motta, M. Nguyen, C. Ochando, P. Paganini, J. Rembser, R. Salerno, U. Sarkar, J. B. Sauvan, Y. Sirois, A. Tarabini, A. Zabi, A. Zghiche

Université de Strasbourg, CNRS, IPHC UMR 7178, Strasbourg, France

J.-L. Agram[18], J. Andrea, D. Apparu, D. Bloch, G. Bourgatte, J.-M. Brom, E. C. Chabert, C. Collard, D. Darej, J.-C. Fontaine[18], U. Goerlach, C. Grimault, A.-C. Le Bihan, E. Nibigira, P. Van Hove

Institut de Physique des 2 Infinis de Lyon (IP2I), Villeurbanne, France

E. Asilar, S. Beauceron, C. Bernet, G. Boudoul, C. Camen, A. Carle, N. Chanon, D. Contardo, P. Depasse, H. El Mamouni, J. Fay, S. Gascon, M. Gouzevitch, B. Ille, I. B. Laktineh, H. Lattaud, A. Lesauvage, M. Lethuillier, L. Mirabito, S. Perries, K. Shchablo, V. Sordini, L. Torterotot, G. Touquet, M. Vander Donckt, S. Viret

Georgian Technical University, Tbilisi, Georgia

I. Lomidze, T. Toriashvili[19], Z. Tsamalaidze[13]

RWTH Aachen University, I. Physikalisches Institut, Aachen, Germany

V. Botta, L. Feld, K. Klein, M. Lipinski, D. Meuser, A. Pauls, N. Röwert, J. Schulz, M. Teroerde

RWTH Aachen University, III. Physikalisches Institut A, Aachen, Germany

A. Dodonova, D. Eliseev, M. Erdmann, P. Fackeldey, B. Fischer, S. Ghosh, T. Hebbeker, K. Hoepfner, F. Ivone, L. Mastrolorenzo, M. Merschmeyer, A. Meyer, G. Mocellin, S. Mondal, S. Mukherjee, D. Noll, A. Novak, T. Pook, A. Pozdnyakov, Y. Rath, H. Reithler, J. Roemer, A. Schmidt, S. C. Schuler, A. Sharma, L. Vigilante, S. Wiedenbeck, S. Zaleski

RWTH Aachen University, III. Physikalisches Institut B, Aachen, Germany

C. Dziwok, G. Flügge, W. Haj Ahmad[20], O. Hlushchenko, T. Kress, A. Nowack, C. Pistone, O. Pooth, D. Roy, H. Sert, A. Stahl[21], T. Ziemons, A. Zotz

Deutsches Elektronen-Synchrotron, Hamburg, Germany

H. Aarup Petersen, M. Aldaya Martin, P. Asmuss, S. Baxter, M. Bayatmakou, O. Behnke, A. Bermúdez Martínez, S. Bhattacharya, A. A. Bin Anuar, K. Borras[22], D. Brunner, A. Campbell, A. Cardini, C. Cheng, F. Colombina, S. Consuegra Rodríguez, G. Correia Silva, V. Danilov, M. De Silva, L. Didukh, G. Eckerlin, D. Eckstein, L. I. Estevez Banos, O. Filatov, E. Gallo[23], A. Geiser, A. Giraldi, A. Grohsjean, M. Guthoff, A. Jafari[24], N. Z. Jomhari, H. Jung, A. Kasem[22], M. Kasemann, H. Kaveh, C. Kleinwort, R. Kogler, D. Krücker, W. Lange, J. Lidrych, K. Lipka, W. Lohmann[25], R. Mankel, I.-A. Melzer-Pellmann, M. Mendizabal Morentin, J. Metwally, A. B. Meyer, M. Meyer, J. Mnich, A. Mussgiller, Y. Otarid, D. Pérez Adán, D. Pitzl, A. Raspereza, B. Ribeiro Lopes, J. Rübenach, A. Saggio, A. Saibel, M. Savitskyi, M. Scham[26], V. Scheurer, S. Schnake, P. Schütze, C. Schwanenberger[23], M. Shchedrolosiev, R. E. Sosa Ricardo, D. Stafford, N. Tonon, M. Van De Klundert, R. Walsh, D. Walter, Q. Wang, Y. Wen, K. Wichmann, L. Wiens, C. Wissing, S. Wuchterl

University of Hamburg, Hamburg, Germany

R. Aggleton, S. Albrecht, S. Bein, L. Benato, P. Connor, K. De Leo, M. Eich, F. Feindt, A. Fröhlich, C. Garbers, E. Garutti, P. Gunnellini, M. Hajheidari, J. Haller, A. Hinzmann, G. Kasieczka, R. Klanner, T. Kramer, V. Kutzner, J. Lange, T. Lange, A. Lobanov, A. Malara, A. Nigamova, K. J. Pena Rodriguez, O. Rieger, P. Schleper, M. Schröder, J. Schwandt, J. Sonneveld, H. Stadie, G. Steinbrück, A. Tews, I. Zoi

Karlsruher Institut fuer Technologie, Karlsruhe, Germany
J. Bechtel, S. Brommer, M. Burkart, E. Butz [iD], R. Caspart, T. Chwalek, W. De Boer[†], A. Dierlamm, A. Droll,
K. El Morabit, N. Faltermann [iD], M. Giffels, J.o. Gosewisch, A. Gottmann, F. Hartmann [iD][21], C. Heidecker,
U. Husemann [iD], P. Keicher, R. Koppenhöfer, S. Maier, M. Metzler, S. Mitra [iD], Th. Müller, M. Neukum, A. Nürnberg,
G. Quast [iD], K. Rabbertz [iD], J. Rauser, D. Savoiu, M. Schnepf, D. Seith, I. Shvetsov, H. J. Simonis, R. Ulrich [iD],
J. Van Der Linden, R. F. Von Cube, M. Wassmer, M. Weber, S. Wieland, R. Wolf, S. Wozniewski, S. Wunsch

Institute of Nuclear and Particle Physics (INPP), NCSR Demokritos, Aghia Paraskevi, Greece
G. Anagnostou, G. Daskalakis, T. Geralis, A. Kyriakis, D. Loukas, A. Stakia

National and Kapodistrian University of Athens, Athens, Greece
M. Diamantopoulou, D. Karasavvas, G. Karathanasis, P. Kontaxakis, C. K. Koraka, A. Manousakis-Katsikakis,
A. Panagiotou, I. Papavergou, N. Saoulidou, K. Theofilatos, E. Tziaferi, K. Vellidis, E. Vourliotis

National Technical University of Athens, Athens, Greece
G. Bakas, K. Kousouris [iD], I. Papakrivopoulos, G. Tsipolitis, A. Zacharopoulou

University of Ioánnina, Ioannina, Greece
K. Adamidis, I. Bestintzanos, I. Evangelou, C. Foudas, P. Gianneios, P. Katsoulis, P. Kokkas, N. Manthos, I. Papadopoulos,
J. Strologas [iD]

MTA-ELTE Lendület CMS Particle and Nuclear Physics Group, Eötvös Loránd University, Budapest, Hungary
M. Csanad [iD], K. Farkas, M. M. A. Gadallah[27], S. Lökös[28], P. Major, K. Mandal, A. Mehta [iD], G. Pasztor [iD], A. J. Rádl,
O. Surányi, G. I. Veres [iD]

Wigner Research Centre for Physics, Budapest, Hungary
M. Bartók [iD][29], G. Bencze, C. Hajdu [iD], D. Horvath[30], F. Sikler [iD], V. Veszpremi

Institute of Nuclear Research ATOMKI, Debrecen, Hungary
S. Czellar, D. Fasanella [iD], J. Karancsi[29], J. Molnar, Z. Szillasi, D. Teyssier

Institute of Physics, University of Debrecen, Debrecen, Hungary
P. Raics, Z. L. Trocsanyi [iD][31], B. Ujvari

Karoly Robert Campus, MATE Institute of Technology, Bengaluru, India
T. Csorgo[32], F. Nemes[32], T. Novak

Indian Institute of Science (IISc), Bangalore, India
S. Choudhury, J. R. Komaragiri [iD], D. Kumar, L. Panwar, P. C. Tiwari

National Institute of Science Education and Research, HBNI, Bhubaneswar, India
S. Bahinipati[33], C. Kar, P. Mal, T. Mishra, V. K. Muraleedharan Nair Bindhu[34], A. Nayak[34], P. Saha, N. Sur [iD],
S. K. Swain, D. Vats[34]

Panjab University, Chandigarh, India
S. Bansal [iD], S. B. Beri, V. Bhatnagar, G. Chaudhary, S. Chauhan, N. Dhingra[35], R. Gupta, A. Kaur, M. Kaur, S. Kaur,
P. Kumari, M. Meena, K. Sandeep, J. B. Singh, A. K. Virdi

University of Delhi, Delhi, India
A. Ahmed, A. Bhardwaj, B. C. Choudhary [iD], M. Gola, S. Keshri [iD], A. Kumar, M. Naimuddin [iD], P. Priyanka, K. Ranjan,
A. Shah [iD]

Saha Institute of Nuclear Physics, HBNI, Kolkata, India
M. Bharti[36], R. Bhattacharya, S. Bhattacharya [iD], D. Bhowmik, S. Dutta, S. Dutta, B. Gomber[37], M. Maity[38], P. Palit,
P. K. Rout, G. Saha, B. Sahu, S. Sarkar, M. Sharan, B. Singh[36], S. Thakur[36]

Indian Institute of Technology Madras, Madras, India
P. K. Behera [iD], S. C. Behera, P. Kalbhor, A. Muhammad, R. Pradhan, P. R. Pujahari, A. Sharma, A. K. Sikdar

Bhabha Atomic Research Centre, Mumbai, India
D. Dutta, V. Jha, V. Kumar, D. K. Mishra, K. Naskar[39], P. K. Netrakanti, L. M. Pant, P. Shukla [iD]
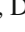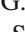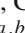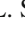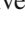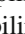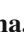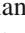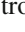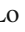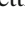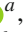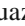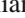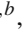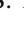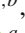
Tata Institute of Fundamental Research-A, Mumbai, India

T. Aziz, S. Dugad, M. Kumar

Tata Institute of Fundamental Research-B, Mumbai, India
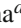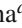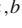
S. Banerjee, R. Chudasama, M. Guchait, S. Karmakar, S. Kumar, G. Majumder, K. Mazumdar, S. Mukherjee

Indian Institute of Science Education and Research (IISER), Pune, India

K. Alpana, S. Dube [iD], B. Kansal, A. Laha, S. Pandey, A. Rane, A. Rastogi, S. Sharma [iD]

Isfahan University of Technology, Isfahan, Iran

H. Bakhshiansohi [iD][40], E. Khazaie, M. Zeinali[41]

Institute for Research in Fundamental Sciences (IPM), Tehran, Iran

S. Chenarani[42], S. M. Etesami, M. Khakzad, M. Mohammadi Najafabadi [iD]

University College Dublin, Dublin, Ireland

M. Grunewald [iD]

INFN Sezione di Bari[a], Università di Bari[b], Politecnico di Bari[c], Bari, Italy

M. Abbrescia [iD][a,b], R. Aly [iD][a,b,43], C. Aruta[a,b], A. Colaleo [iD][a], D. Creanza [iD][a,c], N. De Filippis [iD][a,c], M. De Palma [iD][a,b], A. Di Florio[a,b], A. Di Pilato[a,b], W. Elmetenawee [iD][a,b], L. Fiore [iD][a], A. Gelmi[a,b], M. Gul [iD][a], G. Iaselli [iD][a,c], M. Ince [iD][a,b], S. Lezki [iD][a,b], G. Maggi [iD][a,c], M. Maggi [iD][a], I. Margjeka[a,b], V. Mastrapasqua[a,b], S. My [iD][a,b], S. Nuzzo [iD][a,b], A. Pellecchia[a,b], A. Pompili [iD][a,b], G. Pugliese [iD][a,c], D. Ramos[a], A. Ranieri [iD][a], G. Selvaggi [iD][a,b], L. Silvestris [iD][a], F. M. Simone[a,b], Ü. Sözbilir[a], R. Venditti [iD][a], P. Verwilligen [iD][a]

INFN Sezione di Bologna[a], Università di Bologna[b], Bologna, Italy

G. Abbiendi [iD][a], C. Battilana [iD][a,b], D. Bonacorsi [iD][a,b], L. Borgonovi[a], L. Brigliadori[a], R. Campanini [iD][a,b], P. Capiluppi [iD][a,b], A. Castro [iD][a,b], F. R. Cavallo [iD][a], M. Cuffiani [iD][a,b], G. M. Dallavalle [iD][a], T. Diotalevi[a,b], F. Fabbri [iD][a], A. Fanfani [iD][a,b], P. Giacomelli [iD][a], L. Giommi[a,b], C. Grandi [iD][a], L. Guiducci[a,b], S. Lo Meo[a,44], L. Lunerti[a,b], S. Marcellini [iD][a], G. Masetti [iD][a], F. L. Navarria [iD][a,b], A. Perrotta [iD][a], F. Primavera [iD][a,b], A. M. Rossi [iD][a,b], T. Rovelli [iD][a,b], G. P. Siroli [iD][a,b]

INFN Sezione di Catania[a], Università di Catania[b], Catania, Italy

S. Albergo [iD][a,b,45], S. Costa [iD][a,b,45], A. Di Mattia [iD][a], R. Potenza[a,b], A. Tricomi [iD][a,b,45], C. Tuve [iD][a,b]

INFN Sezione di Firenze[a], Università di Firenze[b], Firenze, Italy

G. Barbagli [iD][a], A. Cassese [iD][a], R. Ceccarelli[a,b], V. Ciulli [iD][a,b], C. Civinini [iD][a], R. D'Alessandro [iD][a,b], E. Focardi [iD][a,b], G. Latino [iD][a,b], P. Lenzi [iD][a,b], M. Lizzo[a,b], M. Meschini [iD][a], S. Paoletti [iD][a], R. Seidita[a,b], G. Sguazzoni [iD][a], L. Viliani [iD][a]

INFN Laboratori Nazionali di Frascati, Frascati, Italy

L. Benussi [iD], S. Bianco [iD], D. Piccolo [iD]

INFN Sezione di Genova[a], Università di Genova[b], Genoa, Italy

M. Bozzo [iD][a,b], F. Ferro [iD][a], R. Mulargia[a,b], E. Robutti [iD][a], S. Tosi [iD][a,b]

INFN Sezione di Milano-Bicocca[a], Università di Milano-Bicocca[b], Milan, Italy

A. Benaglia [iD][a], G. Boldrini, F. Brivio[a,b], F. Cetorelli[a,b], F. De Guio [iD][a,b], M. E. Dinardo [iD][a,b], P. Dini [iD][a], S. Gennai [iD][a], A. Ghezzi [iD][a,b], P. Govoni [iD][a,b], L. Guzzi[a,b], M. T. Lucchini [iD][a,b], M. Malberti[a], S. Malvezzi [iD][a], A. Massironi [iD][a], D. Menasce [iD][a], L. Moroni [iD][a], M. Paganoni [iD][a,b], D. Pedrini [iD][a], B. S. Pinolini, S. Ragazzi [iD][a,b], N. Redaelli [iD][a], T. Tabarelli de Fatis [iD][a,b], D. Valsecchi [iD][a,b,21], D. Zuolo [iD][a,b]

INFN Sezione di Napoli[a], Università di Napoli 'Federico II'[b], Napoli, Italy, Università della Basilicata [c], Potenza, Italy, Università G. Marconi[d], Rome, Italy

S. Buontempo [iD][a], F. Carnevali[a,b], N. Cavallo [iD][a,c], A. De Iorio[a,b], F. Fabozzi [iD][a,c], A. O. M. Iorio [iD][a,b], L. Lista [iD][a,b], S. Meola [iD][a,d,21], P. Paolucci [iD][a,21], B. Rossi [iD][a], C. Sciacca [iD][a,b]

INFN Sezione di Padova[a], Università di Padova[b], Padova, Italy, Università di Trento[c], Trento, Italy

P. Azzi [a], N. Bacchetta [a], D. Bisello [a,b], P. Bortignon [a], A. Bragagnolo[a,b], R. Carlin [a,b], P. Checchia [a], T. Dorigo [a], U. Dosselli [a], F. Gasparini [a,b], U. Gasparini [a,b], G. Grosso, S. Y. Hoh [a,b], L. Layer[a,46], E. Lusiani, M. Margoni [a,b], A. T. Meneguzzo [a,b], J. Pazzini [a,b], P. Ronchese [a,b], R. Rossin[a,b], F. Simonetto [a,b], G. Strong[a], M. Tosi [a,b], H. Yarar[a,b], M. Zanetti [a,b], P. Zotto [a,b], A. Zucchetta [a,b], G. Zumerle [a,b]
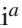
INFN Sezione di Pavia[a], Università di Pavia[b], Pavia, Italy

C. Aime'[a,b], A. Braghieri [a], S. Calzaferri[a,b], D. Fiorina[a,b], P. Montagna[a,b], S. P. Ratti[a,b], V. Re [a], C. Riccardi [a,b], P. Salvini [a], I. Vai [a], P. Vitulo [a,b]
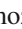
INFN Sezione di Perugia[a], Università di Perugia[b], Perugia, Italy

P. Asenov[a,47], G. M. Bilei [a], D. Ciangottini [a,b], L. Fanò [a,b], P. Lariccia[a,b], M. Magherini[b], G. Mantovani[a,b], V. Mariani[a,b], M. Menichelli [a], F. Moscatelli [a,47], A. Piccinelli[a,b], M. Presilla[a,b], A. Rossi [a,b], A. Santocchia [a,b], D. Spiga [a], T. Tedeschi[a,b]
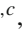
INFN Sezione di Pisa[a], Università di Pisa[b], Scuola Normale Superiore di Pisa[c], Pisa Italy, Università di Siena[d], Siena, Italy

P. Azzurri [a], G. Bagliesi [a], V. Bertacchi[a,c], L. Bianchini [a], T. Boccali [a], E. Bossini[a,b], R. Castaldi [a], M. A. Ciocci [a,b], V. D'Amante[a,d], R. Dell'Orso [a], M. R. Di Domenico[a,d], S. Donato [a], A. Giassi [a], F. Ligabue [a,c], E. Manca [a,c], G. Mandorli[a,c], D. Matos Figueiredo, A. Messineo [a,b], F. Palla [a], S. Parolia[a,b], G. Ramirez-Sanchez[a,c], A. Rizzi [a,b], G. Rolandi [a,c], S. Roy Chowdhury[a,c], A. Scribano[a], N. Shafiei[a,b], P. Spagnolo [a], R. Tenchini [a], G. Tonelli [a,b], N. Turini[a,d], A. Venturi [a], P. G. Verdini [a]

INFN Sezione di Roma[a], Sapienza Università di Roma[b], Rome, Italy

P. Barria [a], M. Campana[a,b], F. Cavallari [a], D. Del Re [a,b], E. Di Marco [a], M. Diemoz [a], E. Longo [a,b], P. Meridiani [a], G. Organtini [a,b], F. Pandolfi[a], R. Paramatti [a,b], C. Quaranta[a,b], S. Rahatlou [a,b], C. Rovelli [a], F. Santanastasio [a,b], L. Soffi [a], R. Tramontano[a,b]
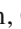
INFN Sezione di Torino[a], Università di Torino[b], Torino, Italy, Università del Piemonte Orientale[c], Novara, Italy

N. Amapane [a,b], R. Arcidiacono [a,c], S. Argiro [a,b], M. Arneodo [a,c], N. Bartosik[a], R. Bellan [a,b], A. Bellora[a,b], J. Berenguer Antequera[a,b], C. Biino [a], N. Cartiglia [a], S. Cometti [a], M. Costa [a,b], R. Covarelli [a,b], N. Demaria [a], B. Kiani[a,b], F. Legger[a], C. Mariotti [a], S. Maselli [a], E. Migliore [a,b], E. Monteil [a,b], M. Monteno [a], M. M. Obertino [a,b], G. Ortona [a], L. Pacher [a,b], N. Pastrone [a], M. Pelliccioni [a], G. L. Pinna Angioni[a,b], M. Ruspa [a,c], K. Shchelina[a], F. Siviero[a,b], V. Sola [a], A. Solano[a,b], D. Soldi [a,b], A. Staiano [a], M. Tornago[a,b], D. Trocino [a], A. Vagnerini[a,b]

INFN Sezione di Trieste[a], Università di Trieste[b], Trieste, Italy

S. Belforte [a], V. Candelise [a,b], M. Casarsa [a], F. Cossutti [a], A. Da Rold [a,b], G. Della Ricca [a,b], G. Sorrentino[a,b], F. Vazzoler [a,b]

Kyungpook National University, Daegu, Korea

S. Dogra [], C. Huh, B. Kim, D. H. Kim, G. N. Kim [], J. Kim, J. Lee, S. W. Lee [], C. S. Moon [], Y. D. Oh [], S. I. Pak, B. C. Radburn-Smith, S. Sekmen [], Y. C. Yang
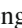
Chonnam National University, Institute for Universe and Elementary Particles, Kwangju, Korea

H. Kim, D. H. Moon []

Hanyang University, Seoul, Korea

B. Francois, T. J. Kim [], J. Park

Korea University, Seoul, Korea

S. Cho, S. Choi [], Y. Go, B. Hong [], K. Lee, K. S. Lee, J. Lim, J. Park, S. K. Park, J. Yoo

Department of Physics, Kyung Hee University, Seoul, Republic of Korea

J. Goh [], A. Gurtu

Sejong University, Seoul, Korea
H. S. Kim, Y. Kim

Seoul National University, Seoul, Korea
J. Almond, J. H. Bhyun, J. Choi, S. Jeon, J. Kim, J. S. Kim, S. Ko, H. Kwon, H. Lee, S. Lee, B. H. Oh, M. Oh, S. B. Oh, H. Seo, U. K. Yang, I. Yoon

University of Seoul, Seoul, Korea
W. Jang, D. Y. Kang, Y. Kang, S. Kim, B. Ko, J. S. H. Lee, Y. Lee, J. A. Merlin, I. C. Park, Y. Roh, M. S. Ryu, D. Song, I. J. Watson, S. Yang

Department of Physics, Yonsei University, Seoul, Korea
S. Ha, H. D. Yoo

Sungkyunkwan University, Suwon, Korea
M. Choi, H. Lee, Y. Lee, I. Yu

College of Engineering and Technology, American University of the Middle East (AUM), Egaila, Kuwait
T. Beyrouthy, Y. Maghrbi

Riga Technical University, Riga, Latvia
K. Dreimanis, V. Veckalns [48]

Vilnius University, Vilnius, Lithuania
M. Ambrozas, A. Carvalho Antunes De Oliveira, A. Juodagalvis, A. Rinkevicius, G. Tamulaitis

National Centre for Particle Physics, Universiti Malaya, Kuala Lumpur, Malaysia
N. Bin Norjoharuddeen, W. A. T. Wan Abdullah, M. N. Yusli, Z. Zolkapli

Universidad de Sonora (UNISON), Hermosillo, Mexico
J. F. Benitez, A. Castaneda Hernandez, M. León Coello, J. A. Murillo Quijada, A. Sehrawat, L. Valencia Palomo

Centro de Investigacion y de Estudios Avanzados del IPN, Mexico City, Mexico
G. Ayala, H. Castilla-Valdez, E. De La Cruz-Burelo, I. Heredia-De La Cruz [49], R. Lopez-Fernandez, C. A. Mondragon Herrera, D. A. Perez Navarro, A. Sanchez-Hernandez

Universidad Iberoamericana, Mexico City, Mexico
S. Carrillo Moreno, C. Oropeza Barrera, F. Vazquez Valencia

Benemerita Universidad Autonoma de Puebla, Puebla, Mexico
I. Pedraza, H. A. Salazar Ibarguen, C. Uribe Estrada

University of Montenegro, Podgorica, Montenegro
J. Mijuskovic [50], N. Raicevic

University of Auckland, Auckland, New Zealand
D. Krofcheck

University of Canterbury, Christchurch, New Zealand
P. H. Butler

National Centre for Physics, Quaid-I-Azam University, Islamabad, Pakistan
A. Ahmad, M. I. Asghar, A. Awais, M. I. M. Awan, H. R. Hoorani, W. A. Khan, M. A. Shah, M. Shoaib, M. Waqas

AGH University of Science and Technology Faculty of Computer Science, Electronics and Telecommunications, Kraków, Poland
V. Avati, L. Grzanka, M. Malawski

National Centre for Nuclear Research, Swierk, Poland
H. Bialkowska, M. Bluj, B. Boimska, M. Górski, M. Kazana, M. Szleper, P. Zalewski

Institute of Experimental Physics, Faculty of Physics, University of Warsaw, Warsaw, Poland
K. Bunkowski, K. Doroba, A. Kalinowski, M. Konecki, J. Krolikowski

Laboratório de Instrumentação e Física Experimental de Partículas, Lisbon, Portugal
M. Araujo, P. Bargassa, D. Bastos, A. Boletti, P. Faccioli, M. Gallinaro, J. Hollar, N. Leonardo, T. Niknejad,
M. Pisano, J. Seixas, O. Toldaiev, J. Varela

Joint Institute for Nuclear Research, Dubna, Russia
S. Afanasiev, D. Budkouski, I. Golutvin, I. Gorbunov, V. Karjavine, V. Korenkov, A. Lanev, A. Malakhov,
V. Matveev[51,52], V. Palichik, V. Perelygin, M. Savina, D. Seitova, V. Shalaev, S. Shmatov, S. Shulha, V. Smirnov,
O. Teryaev, N. Voytishin, B. S. Yuldashev[53], A. Zarubin, I. Zhizhin

Petersburg Nuclear Physics Institute, Gatchina (St. Petersburg), Russia
G. Gavrilov, V. Golovtcov, Y. Ivanov, V. Kim[54], E. Kuznetsova[55], V. Murzin, V. Oreshkin, I. Smirnov, D. Sosnov,
V. Sulimov, L. Uvarov, S. Volkov, A. Vorobyev

Institute for Nuclear Research, Moscow, Russia
Yu. Andreev, A. Dermenev, S. Gninenko, N. Golubev, A. Karneyeu, D. Kirpichnikov, M. Kirsanov, N. Krasnikov,
A. Pashenkov, G. Pivovarov, A. Toropin

Institute for Theoretical and Experimental Physics named by A.I. Alikhanov of NRC 'Kurchatov Institute', Moscow, Russia
V. Epshteyn, V. Gavrilov, N. Lychkovskaya, A. Nikitenko[56], V. Popov, A. Stepennov, M. Toms, E. Vlasov, A. Zhokin

Moscow Institute of Physics and Technology, Moscow, Russia
T. Aushev

National Research Nuclear University 'Moscow Engineering Physics Institute' (MEPhI), Moscow, Russia
O. Bychkova, R. Chistov[57], M. Danilov[58], A. Oskin, P. Parygin, S. Polikarpov[58]

P.N. Lebedev Physical Institute, Moscow, Russia
V. Andreev, M. Azarkin, I. Dremin, M. Kirakosyan, A. Terkulov

Skobeltsyn Institute of Nuclear Physics, Lomonosov Moscow State University, Moscow, Russia
A. Belyaev, E. Boos, V. Bunichev, M. Dubinin[59], L. Dudko, A. Gribushin, V. Klyukhin, O. Kodolova,
I. Lokhtin, S. Obraztsov, S. Petrushanko, V. Savrin, A. Snigirev

Novosibirsk State University (NSU), Novosibirsk, Russia
V. Blinov[60], T. Dimova[60], L. Kardapoltsev[60], A. Kozyrev[60], I. Ovtin[60], O. Radchenko[60], Y. Skovpen[60]

Institute for High Energy Physics of National Research Centre 'Kurchatov Institute', Protvino, Russia
I. Azhgirey, I. Bayshev, D. Elumakhov, V. Kachanov, D. Konstantinov, P. Mandrik, V. Petrov, R. Ryutin,
S. Slabospitskii, A. Sobol, S. Troshin, N. Tyurin, A. Uzunian, A. Volkov

National Research Tomsk Polytechnic University, Tomsk, Russia
A. Babaev, V. Okhotnikov

Tomsk State University, Tomsk, Russia
V. Borshch, V. Ivanchenko, E. Tcherniaev

University of Belgrade: Faculty of Physics and VINCA Institute of Nuclear Sciences, Belgrade, Serbia
P. Adzic[61], M. Dordevic, P. Milenovic, J. Milosevic
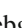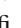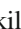
Centro de Investigaciones Energéticas Medioambientales y Tecnológicas (CIEMAT), Madrid, Spain
M. Aguilar-Benitez, J. Alcaraz Maestre, A. Álvarez Fernández, I. Bachiller, M. Barrio Luna, Cristina F. Bedoya,
C. A. Carrillo Montoya, M. Cepeda, M. Cerrada, N. Colino, B. De La Cruz, A. Delgado Peris,
J. P. Fernández Ramos, J. Flix, M. C. Fouz, O. Gonzalez Lopez, S. Goy Lopez, J. M. Hernandez, M. I. Josa,
J. León Holgado, D. Moran, Á. Navarro Tobar, C. Perez Dengra, A. Pérez-Calero Yzquierdo, J. Puerta Pelayo,
I. Redondo, L. Romero, S. Sánchez Navas, L. Urda Gómez, C. Willmott

Universidad Autónoma de Madrid, Madrid, Spain
J. F. de Trocóniz, R. Reyes-Almanza

Instituto Universitario de Ciencias y Tecnologías Espaciales de Asturias (ICTEA), Universidad de Oviedo, Oviedo, Spain
B. Alvarez Gonzalez, J. Cuevas , C. Erice, J. Fernandez Menendez , S. Folgueras , I. Gonzalez Caballero ,
J. R. González Fernández, E. Palencia Cortezon , C. Ramón Álvarez, V. Rodríguez Bouza , A. Soto Rodríguez,
A. Trapote, N. Trevisani , C. Vico Villalba

Instituto de Física de Cantabria (IFCA), CSIC-Universidad de Cantabria, Santander, Spain
J. A. Brochero Cifuentes , I. J. Cabrillo, A. Calderon , J. Duarte Campderros , M. Fernandez ,
C. Fernandez Madrazo, P. J. Fernández Manteca , A. García Alonso, G. Gomez, C. Martinez Rivero,
P. Martinez Ruiz del Arbol , F. Matorras , Pablo Matorras-Cuevas, J. Piedra Gomez , C. Prieels, T. Rodrigo ,
A. Ruiz-Jimeno , L. Scodellaro , I. Vila, J. M. Vizan Garcia

University of Colombo, Colombo, Sri Lanka
M. K. Jayananda, B. Kailasapathy[62], D. U. J. Sonnadara, D. D. C. Wickramarathna

Department of Physics, University of Ruhuna, Matara, Sri Lanka
W. G. D. Dharmaratna , K. Liyanage, N. Perera, N. Wickramage

CERN, European Organization for Nuclear Research, Geneva, Switzerland
T. K. Aarrestad, D. Abbaneo, J. Alimena , E. Auffray, G. Auzinger, J. Baechler, P. Baillon[†], D. Barney, J. Bendavid,
M. Bianco , A. Bocci, T. Camporesi, M. Capeans Garrido, G. Cerminara, N. Chernyavskaya, S. S. Chhibra ,
M. Cipriani , L. Cristella , D. d'Enterria , A. Dabrowski, A. David , A. De Roeck , M. M. Defranchis, M. Deile,
M. Dobson, M. Dünser , N. Dupont, A. Elliott-Peisert, N. Emriskova, F. Fallavollita[63], A. Florent , G. Franzoni ,
W. Funk, S. Giani, D. Gigi, K. Gill, F. Glege, L. Gouskos, M. Haranko , J. Hegeman , V. Innocente, T. James,
P. Janot , J. Kaspar, J. Kieseler , M. Komm , N. Kratochwil, C. Lange , S. Laurila, P. Lecoq , A. Lintuluoto,
K. Long, C. Lourenço , B. Maier, L. Malgeri , S. Mallios, M. Mannelli, A. C. Marini , F. Meijers, S. Mersi ,
E. Meschi , F. Moortgat , M. Mulders , S. Orfanelli, L. Orsini, F. Pantaleo , L. Pape, E. Perez, M. Peruzzi,
A. Petrilli, G. Petrucciani , A. Pfeiffer , M. Pierini , D. Piparo, M. Pitt, H. Qu , T. Quast, D. Rabady , A. Racz,
G. Reales Gutiérrez, M. Rieger , M. Rovere, H. Sakulin, J. Salfeld-Nebgen , S. Scarfi, C. Schäfer, C. Schwick,
M. Selvaggi, A. Sharma, P. Silva , W. Snoeys , P. Sphicas [64], S. Summers, K. Tatar , V. R. Tavolaro , D. Treille,
P. Tropea, A. Tsirou, G. P. Van Onsem , J. Wanczyk[65], K. A. Wozniak, W. D. Zeuner

Paul Scherrer Institut, Villigen, Switzerland
L. Caminada [66], A. Ebrahimi , W. Erdmann, R. Horisberger, Q. Ingram, H. C. Kaestli, D. Kotlinski, U. Langenegger,
M. Missiroli [66], L. Noehte[66], T. Rohe

ETH Zurich-Institute for Particle Physics and Astrophysics (IPA), Zurich, Switzerland
K. Androsov [65], M. Backhaus , P. Berger, A. Calandri, A. De Cosa, G. Dissertori , M. Dittmar, M. Donegà,
C. Dorfer, F. Eble, K. Gedia, F. Glessgen, T. A. Gómez Espinosa , C. Grab , D. Hits, W. Lustermann, A.-M. Lyon,
R. A. Manzoni , L. Marchese, C. Martin Perez, M. T. Meinhard, F. Nessi-Tedaldi, J. Niedziela , F. Pauss, V. Perovic,
S. Pigazzini , M. G. Ratti , M. Reichmann, C. Reissel, T. Reitenspiess, B. Ristic, D. Ruini, D. A. Sanz Becerra,
V. Stampf, J. Steggemann [65], R. Wallny , D. H. Zhu

Universität Zürich, Zurich, Switzerland
C. Amsler[67], P. Bärtschi, C. Botta , D. Brzhechko, M. F. Canelli , K. Cormier, A. De Wit , R. Del Burgo,
J. K. Heikkilä , M. Huwiler, W. Jin, A. Jofrehei, B. Kilminster , S. Leontsinis , S. P. Liechti, A. Macchiolo,
P. Meiring, V. M. Mikuni, U. Molinatti, I. Neutelings, A. Reimers, P. Robmann, S. Sanchez Cruz , K. Schweiger ,
M. Senger, Y. Takahashi

National Central University, Chung-Li, Taiwan
C. Adloff[68], C. M. Kuo, W. Lin, A. Roy, T. Sarkar [38], S. S. Yu

National Taiwan University (NTU), Taipei, Taiwan
L. Ceard, Y. Chao, K. F. Chen, P. H. Chen, W.-S. Hou ⓘ, Y.y. Li, R.-S. Lu, E. Paganis, A. Psallidas, A. Steen, H.y. Wu,
E. Yazgan ⓘ, P.r. Yu

Department of Physics, Faculty of Science, Chulalongkorn University, Bangkok, Thailand
B. Asavapibhop ⓘ, C. Asawatangtrakuldee, N. Srimanobhas

Physics Department, Science and Art Faculty, Çukurova University, Adana, Turkey
F. Boran, S. Damarseckin[69], Z. S. Demiroglu ⓘ, F. Dolek, I. Dumanoglu[70], E. Eskut, Y. Guler[71], E. Gurpinar Guler[71],
C. Isik, O. Kara, A. Kayis Topaksu, U. Kiminsu ⓘ, G. Onengut, K. Ozdemir[72], A. Polatoz, A. E. Simsek, B. Tali[73],
U. G. Tok, S. Turkcapar, I. S. Zorbakir ⓘ

Physics Department, Middle East Technical University, Ankara, Turkey
B. Isildak[74], G. Karapinar, K. Ocalan ⓘ[75], M. Yalvac[76]

Bogazici University, Istanbul, Turkey
B. Akgun, I. O. Atakisi, E. Gülmez ⓘ, M. Kaya[77], O. Kaya[78], Ö. Özçelik, S. Tekten[79], E. A. Yetkin ⓘ[80]

Istanbul Technical University, Istanbul, Turkey
A. Cakir ⓘ, K. Cankocak[70], Y. Komurcu, S. Sen ⓘ[81]

Istanbul University, Istanbul, Turkey
S. Cerci[73], I. Hos[82], B. Kaynak, S. Ozkorucuklu, D. Sunar Cerci[73], C. Zorbilmez

Institute for Scintillation Materials of National Academy of Science of Ukraine, Kharkov, Ukraine
B. Grynyov

National Scientific Center, Kharkov Institute of Physics and Technology, Kharkov, Ukraine
L. Levchuk ⓘ
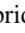
University of Bristol, Bristol, UK
D. Anthony, E. Bhal, S. Bologna, J. J. Brooke ⓘ, A. Bundock ⓘ, E. Clement ⓘ, D. Cussans, H. Flacher ⓘ, J. Goldstein ⓘ,
G. P. Heath, H. F. Heath ⓘ, L. Kreczko ⓘ, B. Krikler ⓘ, S. Paramesvaran, S. Seif El Nasr-Storey, V. J. Smith,
N. Stylianou[83], K. Walkingshaw Pass, R. White

Rutherford Appleton Laboratory, Didcot, UK
K. W. Bell, A. Belyaev ⓘ[84], C. Brew ⓘ, R. M. Brown, D. J. A. Cockerill, C. Cooke, K. V. Ellis, K. Harder, S. Harper,
M.l. Holmberg[85], J. Linacre ⓘ, K. Manolopoulos, D. M. Newbold ⓘ, E. Olaiya, D. Petyt, T. Reis ⓘ, T. Schuh,
C. H. Shepherd-Themistocleous, I. R. Tomalin, T. Williams

Imperial College, London, UK
R. Bainbridge ⓘ, P. Bloch, S. Bonomally, J. Borg ⓘ, S. Breeze, O. Buchmuller, V. Cepaitis, G. S. Chahal[86], D. Colling,
P. Dauncey ⓘ, G. Davies, M. Della Negra ⓘ, S. Fayer, G. Fedi ⓘ, G. Hall ⓘ, M. H. Hassanshahi, G. Iles, J. Langford,
L. Lyons, A.-M. Magnan, S. Malik, A. Martelli ⓘ, D. G. Monk, J. Nash ⓘ[87], M. Pesaresi, D. M. Raymond, A. Richards,
A. Rose, E. Scott ⓘ, C. Seez, A. Shtipliyski, A. Tapper ⓘ, K. Uchida, T. Virdee ⓘ[21], M. Vojinovic ⓘ, N. Wardle ⓘ,
S. N. Webb, D. Winterbottom

Brunel University, Uxbridge, UK
K. Coldham, J. E. Cole ⓘ, A. Khan, P. Kyberd ⓘ, I. D. Reid ⓘ, L. Teodorescu, S. Zahid

Baylor University, Waco, USA
S. Abdullin ⓘ, A. Brinkerhoff ⓘ, B. Caraway, J. Dittmann, K. Hatakeyama, A. R. Kanuganti, B. McMaster, N. Pastika,
M. Saunders, S. Sawant, C. Sutantawibul, J. Wilson

Catholic University of America, Washington, DC, USA
R. Bartek ⓘ, A. Dominguez ⓘ, R. Uniyal, A. M. Vargas Hernandez

The University of Alabama, Tuscaloosa, USA
A. Buccilli ⓘ, S. I. Cooper, D. Di Croce, S. V. Gleyzer, C. Henderson ⓘ, C. U. Perez ⓘ, P. Rumerio[88], C. West

Boston University, Boston, USA

A. Akpinar, A. Albert, D. Arcaro, C. Cosby, Z. Demiragli, E. Fontanesi, D. Gastler, S. May, J. Rohlf, K. Salyer, D. Sperka, D. Spitzbart, I. Suarez, A. Tsatsos, S. Yuan, D. Zou

Brown University, Providence, USA

G. Benelli, B. Burkle, X. Coubez[22], D. Cutts, M. Hadley, U. Heintz, J. M. Hogan[89], T. KWON, G. Landsberg, K. T. Lau, D. Li, M. Lukasik, J. Luo, M. Narain, N. Pervan, S. Sagir[90], F. Simpson, E. Usai, W. Y. Wong, X. Yan, D. Yu, W. Zhang

University of California, Davis, Davis, USA

J. Bonilla, C. Brainerd, R. Breedon, M. Calderon De La Barca Sanchez, M. Chertok, J. Conway, P. T. Cox, R. Erbacher, G. Haza, F. Jensen, O. Kukral, R. Lander, M. Mulhearn, D. Pellett, B. Regnery, D. Taylor, Y. Yao, F. Zhang

University of California, Los Angeles, USA

M. Bachtis, R. Cousins, A. Datta, D. Hamilton, J. Hauser, M. Ignatenko, M. A. Iqbal, T. Lam, W. A. Nash, S. Regnard, D. Saltzberg, B. Stone, V. Valuev

University of California, Riverside, Riverside, USA

K. Burt, Y. Chen, R. Clare, J. W. Gary, M. Gordon, G. Hanson, G. Karapostoli, O. R. Long, N. Manganelli, M. Olmedo Negrete, W. Si, S. Wimpenny, Y. Zhang

University of California, San Diego, La Jolla, USA

J. G. Branson, P. Chang, S. Cittolin, S. Cooperstein, N. Deelen, D. Diaz, J. Duarte, R. Gerosa, L. Giannini, J. Guiang, R. Kansal, V. Krutelyov, R. Lee, J. Letts, M. Masciovecchio, F. Mokhtar, M. Pieri, B. V. Sathia Narayanan, V. Sharma, M. Tadel, A. Vartak, F. Würthwein, Y. Xiang, A. Yagil

Department of Physics, University of California, Santa Barbara, Santa Barbara, USA

N. Amin, C. Campagnari, M. Citron, A. Dorsett, V. Dutta, J. Incandela, M. Kilpatrick, J. Kim, B. Marsh, H. Mei, M. Oshiro, M. Quinnan, J. Richman, U. Sarica, F. Setti, J. Sheplock, D. Stuart, S. Wang

California Institute of Technology, Pasadena, USA

A. Bornheim, O. Cerri, I. Dutta, J. M. Lawhorn, N. Lu, J. Mao, H. B. Newman, T. Q. Nguyen, M. Spiropulu, J. R. Vlimant, C. Wang, S. Xie, Z. Zhang, R. Y. Zhu

Carnegie Mellon University, Pittsburgh, USA

J. Alison, S. An, M. B. Andrews, P. Bryant, T. Ferguson, A. Harilal, C. Liu, T. Mudholkar, M. Paulini, A. Sanchez, W. Terrill
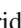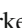
University of Colorado Boulder, Boulder, USA

J. P. Cumalat, W. T. Ford, A. Hassani, E. MacDonald, R. Patel, A. Perloff, C. Savard, K. Stenson, K. A. Ulmer, S. R. Wagner

Cornell University, Ithaca, USA

J. Alexander, S. Bright-thonney, X. Chen, Y. Cheng, D. J. Cranshaw, S. Hogan, J. Monroy, J. R. Patterson, D. Quach, J. Reichert, M. Reid, A. Ryd, W. Sun, J. Thom, P. Wittich, R. Zou

Fermi National Accelerator Laboratory, Batavia, USA

M. Albrow, M. Alyari, G. Apollinari, A. Apresyan, A. Apyan, S. Banerjee, L. A. T. Bauerdick, D. Berry, J. Berryhill, P. C. Bhat, K. Burkett, J. N. Butler, A. Canepa, G. B. Cerati, H. W. K. Cheung, F. Chlebana, K. F. Di Petrillo, V. D. Elvira, Y. Feng, J. Freeman, Z. Gecse, L. Gray, D. Green, S. Grünendahl, O. Gutsche, R. M. Harris, R. Heller, T. C. Herwig, J. Hirschauer, B. Jayatilaka, S. Jindariani, M. Johnson, U. Joshi, T. Klijnsma, B. Klima, K. H. M. Kwok, S. Lammel, D. Lincoln, R. Lipton, T. Liu, C. Madrid, K. Maeshima, C. Mantilla, D. Mason, P. McBride, P. Merkel, S. Mrenna, S. Nahn, J. Ngadiuba, V. O'Dell, V. Papadimitriou, K. Pedro, C. Pena[59], O. Prokofyev, F. Ravera, A. Reinsvold Hall, L. Ristori, E. Sexton-Kennedy, N. Smith, A. Soha, W. J. Spalding, L. Spiegel, S. Stoynev, J. Strait, L. Taylor, S. Tkaczyk, N. V. Tran, L. Uplegger, E. W. Vaandering, H. A. Weber

University of Florida, Gainesville, USA

D. Acosta, P. Avery, D. Bourilkov, L. Cadamuro, V. Cherepanov, F. Errico, R. D. Field, D. Guerrero, B. M. Joshi, M. Kim, E. Koenig, J. Konigsberg, A. Korytov, K. H. Lo, K. Matchev, N. Menendez, G. Mitselmakher, A. Muthirakalayil Madhu, N. Rawal, D. Rosenzweig, S. Rosenzweig, J. Rotter, K. Shi, J. Sturdy, J. Wang, E. Yigitbasi, X. Zuo

Florida State University, Tallahassee, USA

T. Adams, A. Askew, R. Habibullah, V. Hagopian, K. F. Johnson, R. Khurana, T. Kolberg, G. Martinez, H. Prosper, C. Schiber, O. Viazlo, R. Yohay, J. Zhang

Florida Institute of Technology, Melbourne, USA

M. M. Baarmand, S. Butalla, T. Elkafrawy[91], M. Hohlmann, R. Kumar Verma, D. Noonan, M. Rahmani, F. Yumiceva

University of Illinois at Chicago (UIC), Chicago, USA

M. R. Adams, H. Becerril Gonzalez, R. Cavanaugh, S. Dittmer, O. Evdokimov, C. E. Gerber, D. A. Hangal, D. J. Hofman, A. H. Merrit, C. Mills, G. Oh, T. Roy, S. Rudrabhatla, M. B. Tonjes, N. Varelas, J. Viinikainen, X. Wang, Z. Wu, Z. Ye
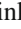
The University of Iowa, Iowa City, USA

M. Alhusseini, K. Dilsiz[92], R. P. Gandrajula, O. K. Köseyan, J.-P. Merlo, A. Mestvirishvili[93], J. Nachtman, H. Ogul[94], Y. Onel, A. Penzo, C. Snyder, E. Tiras[95]

Johns Hopkins University, Baltimore, USA

O. Amram, B. Blumenfeld, L. Corcodilos, J. Davis, M. Eminizer, A. V. Gritsan, S. Kyriacou, P. Maksimovic, J. Roskes, M. Swartz, T. Á. Vámi

The University of Kansas, Lawrence, USA

A. Abreu, J. Anguiano, C. Baldenegro Barrera, P. Baringer, A. Bean, A. Bylinkin, Z. Flowers, T. Isidori, S. Khalil, J. King, G. Krintiras, A. Kropivnitskaya, M. Lazarovits, C. Le Mahieu, C. Lindsey, J. Marquez, N. Minafra, M. Murray, M. Nickel, C. Rogan, C. Royon, R. Salvatico, S. Sanders, E. Schmitz, C. Smith, J. D. Tapia Takaki, Q. Wang, Z. Warner, J. Williams, G. Wilson

Kansas State University, Manhattan, USA

S. Duric, A. Ivanov, K. Kaadze, D. Kim, Y. Maravin, T. Mitchell, A. Modak, K. Nam

Lawrence Livermore National Laboratory, Livermore, USA

F. Rebassoo, D. Wright

University of Maryland, College Park, USA

E. Adams, A. Baden, O. Baron, A. Belloni, S. C. Eno, N. J. Hadley, S. Jabeen, R. G. Kellogg, T. Koeth, A. C. Mignerey, S. Nabili, C. Palmer, M. Seidel, A. Skuja, L. Wang, K. Wong

Massachusetts Institute of Technology, Cambridge, USA

D. Abercrombie, G. Andreassi, R. Bi, W. Busza, I. A. Cali, Y. Chen, M. D'Alfonso, J. Eysermans, C. Freer, G. Gomez Ceballos, M. Goncharov, P. Harris, M. Hu, M. Klute, D. Kovalskyi, J. Krupa, Y.-J. Lee, C. Mironov, C. Paus, D. Rankin, C. Roland, G. Roland, Z. Shi, G. S. F. Stephans, J. Wang, Z. Wang, B. Wyslouch

University of Minnesota, Minneapolis, USA

R. M. Chatterjee, A. Evans, J. Hiltbrand, Sh. Jain, M. Krohn, Y. Kubota, J. Mans, M. Revering, R. Rusack, R. Saradhy, N. Schroeder, N. Strobbe, M. A. Wadud

University of Nebraska-Lincoln, Lincoln, USA

K. Bloom, M. Bryson, S. Chauhan, D. R. Claes, C. Fangmeier, L. Finco, F. Golf, C. Joo, I. Kravchenko, M. Musich, I. Reed, J. E. Siado, G. R. Snow[†], W. Tabb, F. Yan, A. G. Zecchinelli

State University of New York at Buffalo, Buffalo, USA

G. Agarwal, H. Bandyopadhyay, L. Hay, I. Iashvili, A. Kharchilava, C. McLean, D. Nguyen, J. Pekkanen, S. Rappoccio, A. Williams

Northeastern University, Boston, USA

G. Alverson, E. Barberis, Y. Haddad, A. Hortiangtham, J. Li, G. Madigan, B. Marzocchi, D. M. Morse,
V. Nguyen, T. Orimoto, A. Parker, L. Skinnari, A. Tishelman-Charny, T. Wamorkar, B. Wang, A. Wisecarver, D. Wood

Northwestern University, Evanston, USA

S. Bhattacharya, J. Bueghly, Z. Chen, A. Gilbert, T. Gunter, K. A. Hahn, Y. Liu, N. Odell, M. H. Schmitt, M. Velasco

University of Notre Dame, Notre Dame, USA

R. Band, R. Bucci, M. Cremonesi, A. Das, N. Dev, R. Goldouzian, M. Hildreth, K. Hurtado Anampa, C. Jessop,
K. Lannon, J. Lawrence, N. Loukas, D. Lutton, N. Marinelli, I. Mcalister, T. McCauley, C. Mcgrady, K. Mohrman,
C. Moore, Y. Musienko[51], R. Ruchti, P. Siddireddy, A. Townsend, M. Wayne, A. Wightman, M. Zarucki, L. Zygala

The Ohio State University, Columbus, USA

B. Bylsma, B. Cardwell, L. S. Durkin, B. Francis, C. Hill, M. Nunez Ornelas, K. Wei, B. L. Winer, B. R. Yates

Princeton University, Princeton, USA

F. M. Addesa, B. Bonham, P. Das, G. Dezoort, P. Elmer, A. Frankenthal, B. Greenberg, N. Haubrich,
S. Higginbotham, A. Kalogeropoulos, G. Kopp, S. Kwan, D. Lange, D. Marlow, K. Mei, I. Ojalvo, J. Olsen,
D. Stickland, C. Tully

University of Puerto Rico, Mayaguez, USA

S. Malik, S. Norberg

Purdue University, West Lafayette, USA

A. S. Bakshi, V. E. Barnes, R. Chawla, S. Das, L. Gutay, M. Jones, A. W. Jung, S. Karmarkar, D. Kondratyev, M. Liu,
G. Negro, N. Neumeister, G. Paspalaki, S. Piperov, A. Purohit, J. F. Schulte, M. Stojanovic[17], J. Thieman,
F. Wang, R. Xiao, W. Xie

Purdue University Northwest, Hammond, USA

J. Dolen, N. Parashar

Rice University, Houston, USA

A. Baty, T. Carnahan, M. Decaro, S. Dildick, K. M. Ecklund, S. Freed, P. Gardner, F. J. M. Geurts, A. Kumar,
W. Li, B. P. Padley, R. Redjimi, W. Shi, A. G. Stahl Leiton, S. Yang, L. Zhang[96], Y. Zhang

University of Rochester, Rochester, USA

A. Bodek, P. de Barbaro, R. Demina, J. L. Dulemba, C. Fallon, T. Ferbel, M. Galanti, A. Garcia-Bellido, O. Hindrichs,
A. Khukhunaishvili, E. Ranken, R. Taus

Rutgers, The State University of New Jersey, Piscataway, USA

B. Chiarito, J. P. Chou, A. Gandrakota, Y. Gershtein, E. Halkiadakis, A. Hart, M. Heindl, O. Karacheban[25],
I. Laflotte, A. Lath, R. Montalvo, K. Nash, M. Osherson, S. Salur, S. Schnetzer, S. Somalwar, R. Stone,
S. A. Thayil, S. Thomas, H. Wang

University of Tennessee, Knoxville, USA

H. Acharya, A. G. Delannoy, S. Fiorendi, S. Spanier

Texas A&M University, College Station, USA

O. Bouhali[97], M. Dalchenko, A. Delgado, R. Eusebi, J. Gilmore, T. Huang, T. Kamon[98], H. Kim, S. Luo, S. Malhotra,
R. Mueller, D. Overton, D. Rathjens, A. Safonov

Texas Tech University, Lubbock, USA

N. Akchurin, J. Damgov, V. Hegde, S. Kunori, K. Lamichhane, S. W. Lee, T. Mengke, S. Muthumuni, T. Peltola,
I. Volobouev, Z. Wang, A. Whitbeck

Vanderbilt University, Nashville, USA

E. Appelt, S. Greene, A. Gurrola, W. Johns, A. Melo, H. Ni, K. Padeken, F. Romeo, P. Sheldon, S. Tuo, J. Velkovska

University of Virginia, Charlottesville, USA

M. W. Arenton, B. Cox, G. Cummings, J. Hakala, R. Hirosky ⓘ, M. Joyce, A. Ledovskoy, A. Li, C. Neu ⓘ, C. E. Perez Lara, B. Tannenwald ⓘ, S. White ⓘ, E. Wolfe

Wayne State University, Detroit, USA

N. Poudyal ⓘ

University of Wisconsin-Madison, Madison, WI, USA

K. Black, T. Bose, C. Caillol, S. Dasu ⓘ, I. De Bruyn ⓘ, P. Everaerts ⓘ, F. Fienga, C. Galloni, H. He, M. Herndon ⓘ, A. Hervé, U. Hussain, A. Lanaro, A. Loeliger, R. Loveless, J. Madhusudanan Sreekala ⓘ, A. Mallampalli, A. Mohammadi, D. Pinna, A. Savin, V. Shang, V. Sharma ⓘ, W. H. Smith ⓘ, D. Teague, S. Trembath-Reichert, W. Vetens

† **Deceased**

1: Also at TU Wien, Wien, Austria
2: Also at Institute of Basic and Applied Sciences, Faculty of Engineering, Arab Academy for Science, Technology and Maritime Transport, Alexandria, Egypt
3: Also at Université Libre de Bruxelles, Bruxelles, Belgium
4: Also at Universidade Estadual de Campinas, Campinas, Brazil
5: Also at Federal University of Rio Grande do Sul, Porto Alegre, Brazil
6: Also at The University of the State of Amazonas, Manaus, Brazil
7: Also at University of Chinese Academy of Sciences, Beijing, China
8: Also at Department of Physics, Tsinghua University, Beijing, China
9: Also at UFMS, Nova Andradina, Brazil
10: Also at Department of Physics, Nanjing Normal University, Nanjing, China
11: Now at The University of Iowa, Iowa City, USA
12: Also at Institute for Theoretical and Experimental Physics named by A.I. Alikhanov of NRC 'Kurchatov Institute', Moscow, Russia
13: Also at Joint Institute for Nuclear Research, Dubna, Russia
14: Also at Cairo University, Cairo, Egypt
15: Also at Suez University, Suez, Egypt
16: Now at British University in Egypt, Cairo, Egypt
17: Also at Purdue University, West Lafayette, USA
18: Also at Université de Haute Alsace, Mulhouse, France
19: Also at Tbilisi State University, Tbilisi, Georgia
20: Also at Erzincan Binali Yildirim University, Erzincan, Turkey
21: Also at CERN, European Organization for Nuclear Research, Geneva, Switzerland
22: Also at RWTH Aachen University, III. Physikalisches Institut A, Aachen, Germany
23: Also at University of Hamburg, Hamburg, Germany
24: Also at Isfahan University of Technology, Isfahan, Iran
25: Also at Brandenburg University of Technology, Cottbus, Germany
26: Also at Forschungszentrum Jülich, Juelich, Germany
27: Also at Physics Department, Faculty of Science, Assiut University, Assiut, Egypt
28: Also at Karoly Robert Campus, MATE Institute of Technology, Gyongyos, Hungary
29: Also at Institute of Physics, University of Debrecen, Debrecen, Hungary
30: Also at Institute of Nuclear Research ATOMKI, Debrecen, Hungary
31: Also at MTA-ELTE Lendület CMS Particle and Nuclear Physics Group, Eötvös Loránd University, Budapest, Hungary
32: Also at Wigner Research Centre for Physics, Budapest, Hungary
33: Also at IIT Bhubaneswar, Bhubaneswar, India
34: Also at Institute of Physics, Bhubaneswar, India
35: Also at Punjab Agricultural University, Ludhiana, India
36: Also at Shoolini University, Solan, India
37: Also at University of Hyderabad, Hyderabad, India
38: Also at University of Visva-Bharati, Santiniketan, India
39: Also at Indian Institute of Technology (IIT), Mumbai, India

40: Also at Deutsches Elektronen-Synchrotron, Hamburg, Germany

41: Also at Sharif University of Technology, Tehran, Iran

42: Also at Department of Physics, University of Science and Technology of Mazandaran, Behshahr, Iran

43: Now at INFN Sezione di Bari^a, Università di Bari^b, Politecnico di Bari^c, Bari, Italy

44: Also at Italian National Agency for New Technologies, Energy and Sustainable Economic Development, Bologna, Italy

45: Also at Centro Siciliano di Fisica Nucleare e di Struttura Della Materia, Catania, Italy

46: Also at Università di Napoli 'Federico II', Naples, Italy

47: Also at Consiglio Nazionale delle Ricerche-Istituto Officina dei Materiali, Perugia, Italy

48: Also at Riga Technical University, Riga, Latvia

49: Also at Consejo Nacional de Ciencia y Tecnología, Mexico City, Mexico

50: Also at IRFU, CEA, Université Paris-Saclay, Gif-sur-Yvette, France

51: Also at Institute for Nuclear Research, Moscow, Russia

52: Now at National Research Nuclear University 'Moscow Engineering Physics Institute' (MEPhI), Moscow, Russia

53: Also at Institute of Nuclear Physics of the Uzbekistan Academy of Sciences, Tashkent, Uzbekistan

54: Also at St. Petersburg State Polytechnical University, St. Petersburg, Russia

55: Also at University of Florida, Gainesville, USA

56: Also at Imperial College, London, UK

57: Also at Moscow Institute of Physics and Technology, Moscow, Russia

58: Also at P.N. Lebedev Physical Institute, Moscow, Russia

59: Also at California Institute of Technology, Pasadena, USA

60: Also at Budker Institute of Nuclear Physics, Novosibirsk, Russia

61: Also at Faculty of Physics, University of Belgrade, Belgrade, Serbia

62: Also at Trincomalee Campus, Eastern University, Nilaveli, Sri Lanka

63: Also at INFN Sezione di Pavia^a, Università di Pavia^b, Pavia, Italy

64: Also at National and Kapodistrian University of Athens, Athens, Greece

65: Also at Ecole Polytechnique Fédérale Lausanne, Lausanne, Switzerland

66: Also at Universität Zürich, Zurich, Switzerland

67: Also at Stefan Meyer Institute for Subatomic Physics, Vienna, Austria

68: Also at Laboratoire d'Annecy-le-Vieux de Physique des Particules, IN2P3-CNRS, Annecy-le-Vieux, France

69: Also at Şırnak University, Sirnak, Turkey

70: Also at Near East University, Research Center of Experimental Health Science, Nicosia, Turkey

71: Also at Konya Technical University, Konya, Turkey

72: Also at Piri Reis University, Istanbul, Turkey

73: Also at Adiyaman University, Adiyaman, Turkey

74: Also at Ozyegin University, Istanbul, Turkey

75: Also at Necmettin Erbakan University, Konya, Turkey

76: Also at Bozok Universitetesi Rektörlügü, Yozgat, Turkey

77: Also at Marmara University, Istanbul, Turkey

78: Also at Milli Savunma University, Istanbul, Turkey

79: Also at Kafkas University, Kars, Turkey

80: Also at Istanbul Bilgi University, Istanbul, Turkey

81: Also at Hacettepe University, Ankara, Turkey

82: Also at Faculty of Engineering, Istanbul University-Cerrahpasa, Istanbul, Turkey

83: Also at Vrije Universiteit Brussel, Brussel, Belgium

84: Also at School of Physics and Astronomy, University of Southampton, Southampton, UK

85: Also at Rutherford Appleton Laboratory, Didcot, UK

86: Also at IPPP Durham University, Durham, UK

87: Also at Monash University, Faculty of Science, Clayton, Australia

88: Also at Università di Torino, Torino, Italy

89: Also at Bethel University, USA, St. Paul, Minneapolis, USA

90: Also at Karamanoğlu Mehmetbey University, Karaman, Turkey

91: Also at Ain Shams University, Cairo, Egypt

92: Also at Bingol University, Bingol, Turkey

93: Also at Georgian Technical University, Tbilisi, Georgia

94: Also at Sinop University, Sinop, Turkey

95: Also at Erciyes University, Kayseri, Turkey

96: Also at Institute of Modern Physics and Key Laboratory of Nuclear Physics and Ion-beam Application (MOE)-Fudan University, Shanghai, China

97: Also at Texas A&M University at Qatar, Doha, Qatar

98: Also at Kyungpook National University, Daegu, Korea